Towards valorization of pectin-rich agro-industrial residues: Engineering of *Saccharomyces cerevisiae* for co-fermentation of D-galacturonic acid and glycerol

Andreea Perpelea [a], Andy Wiranata Wijaya [a,b], Luís C. Martins [c], Dorthe Rippert [a], Mathias Klein [a], Angel Angelov [d,e], Kaisa Peltonen [f], Attila Teleki [b], Wolfgang Liebl [d], Peter Richard [f], Johan M. Thevelein [g], Ralf Takors [b], Isabel Sá-Correia [c,h], Elke Nevoigt [a,*]

[a] *Department of Life Sciences and Chemistry, Jacobs University Bremen gGmbH, Campus Ring 1, 28759, Bremen, Germany*
[b] *Institute of Biochemical Engineering, University of Stuttgart, Allmandring 31, 70569, Stuttgart, Germany*
[c] *iBB – Institute for Bioengineering and Biosciences/i4HB-Associate Laboratory Institute for Health and Bioeconomy at Instituto Superior Técnico, Universidade de Lisboa, Av. Rovisco Pais, 1049-001, Lisbon, Portugal*
[d] *Chair of Microbiology, TUM School of Life Sciences, Technical University of Munich, Emil-Ramann-Str 4, 85354, Freising-Weihenstephan, Germany*
[e] *NGS Competence Center Tübingen, Universitätsklinikum Tübingen, Calwerstraße 7, 72076, Tübingen, Germany*
[f] *VTT Technical Research Centre of Finland Ltd., P.O. Box 1000, 02044, VTT Espoo, Finland*
[g] *NovelYeast bv, Open Bio-Incubator, Erasmus High School, Laarbeeklaan 121, 1090, Brussels (Jette), Belgium*
[h] *Department of Bioengineering, Instituto Superior Técnico, Universidade de Lisboa, Av. Rovisco Pais, 1049-001, Lisbon, Portugal*

ARTICLE INFO

ABSTRACT

Pectin-rich plant biomass residues represent underutilized feedstocks for industrial biotechnology. The conversion of the oxidized monomer D-galacturonic acid (D-GalUA) to highly reduced fermentation products such as alcohols is impossible due to the lack of electrons. The reduced compound glycerol has therefore been considered an optimal co-substrate, and a cell factory able to efficiently co-ferment these two carbon sources is in demand. Here, we inserted the fungal D-GalUA pathway in a strain of the yeast *S. cerevisiae* previously equipped with an NAD-dependent glycerol catabolic pathway. The constructed strain was able to consume D-GalUA with the highest reported maximum specific rate of 0.23 g g_{CDW}^{-1} h^{-1} in synthetic minimal medium when glycerol was added. By means of a ^{13}C isotope-labelling analysis, carbon from both substrates was shown to end up in pyruvate. The study delivers the proof of concept for a co-fermentation of the two 'respiratory' carbon sources to ethanol and demonstrates a fast and complete consumption of D-GalUA in crude sugar beet pulp hydrolysate under aerobic conditions. The future challenge will be to achieve co-fermentation under industrial, quasi-anaerobic conditions.

1. Introduction

Sustainability envisions a finely balanced integration of economic success, resource availability and affordability, based on environment-friendly practices. It has become clear that our current 'take-make-dispose' production pattern has to be replaced by a circular economy model (Geisendorf and Pietrulla, 2018; Merli et al., 2018). Using feedstocks obtained from biomass-derived agro-industrial waste streams as raw materials for the production of chemicals and fuels can significantly contribute to this concept (Tripathi et al., 2019). The use of biocatalysts, such as enzymes and cells, allows operations close to ambient temperatures and pressures in an aqueous environment, without the production of toxic waste (Burk and van Dien, 2016). Moreover, the development of novel tailor-made bioprocesses supported by synthetic biology and metabolic engineering lies at the forefront of the current advances in industrial biotechnology ("Expanding biocatalysis for a sustainable future," 2020; Nielsen and Keasling, 2016).

Lignocellulosic biomass residues such as corn stover or wheat straw have received much attention as second-generation feedstocks for industrial biotechnology. Less explored agricultural residues with high potential for fermentation-based production processes are pectin-rich biomass streams generated from the sugar industry or the processing of fruits and vegetables. Well-known examples are sugar beet pulp

---

Abbreviations

DHA	dihydroxyacetone
D-GalUA	D-galacturonic acid
L-GalA	L-galactonate
SBP	sugar beet pulp
CPW	citrus processing waste
CDW	cell dry weight

(SBP), citrus processing waste (CPW), and apple pomace (Edwards and Doran-Peterson, 2012). These residues have a very low lignin content and are already partially pre-treated as the result of sugar and juice extraction, facilitating further processing (Berlowska et al., 2018; John et al., 2017). So far, these materials have been used mainly as low-value animal feed or ended up in landfills.

SBP is the most abundant of the three mentioned pectin-rich agro-industrial by-products (Edwards and Doran-Peterson, 2012; "FAOSTAT," n.d.). In Europe alone, the annual sugar beet production exceeded 150 million tonnes for the past decade, even reaching 219 million tonnes in 2017 ("FAOSTAT," n.d.). As 4.6–5% of the sugar beet finally ends up in SBP ("Legrand, 2015. Collection les guides techniques de l'IRBAB | Feedipedia," n.d.), it can be estimated that up to 11 million tonnes of this pectin-containing residue were produced in Europe only in 2017.

As the polymer matrix of pectin has a complex structure, pectin-rich agro-industrial residues pose particular challenges with regard to hydrolysis and fermentation (Müller-Maatsch et al., 2016). The exact composition of the different biomass hydrolysis is highly dependent on the conditions of pre-treatment and enzymatic hydrolysis (Berlowska et al., 2017; Gama et al., 2015; Hamley-Bennett et al., 2016; Martins et al., 2020). However, D-glucose, D-galacturonic acid (D-GalUA), L-arabinose, and D-galactose are quantitatively the most abundant monomers in pectin-rich agro-industrial residues and can serve as carbon sources for microbial cell factories (Valk, 2020). In contrast to neutral sugars, D-GalUA is a weak acid that negatively impacts microbial growth and fermentation, particularly at low pH (Huisjes et al., 2012a; Martins et al., 2020). Moreover, as pectin structures are acetylated, their hydrolysis also releases significant amounts of another weak acid, acetic acid. The concentration of this potent inhibitor of microbial fermentation is higher in SBP hydrolysates compared to those derived from citrus processing wastes (Grohmann et al., 1999; Günan Yücel and Aksu, 2015).

Among potential microorganisms for the fermentation of pectin-rich biomass hydrolysates, the yeast *S. cerevisiae* is highly attractive since it has a relatively high natural tolerance to weak acids (Jeong et al., 2021; Palma et al., 2018). Apart from this, its long-term traditional use in industry, its natural capacity for efficient fermentation under anaerobic conditions supported by high glycolytic fluxes, as well as its extraordinary accessibility for extensive genetic manipulation are other important reasons for its popularity. Although its natural sugar spectrum is limited to hexose sugars, *S. cerevisiae* has still been a highly popular microorganism for fermentation of lignocellulose-based renewable resources (Duwe et al., 2019). Efforts to engineer this organism for the fermentation of pentose sugars as well as for the co-fermentation of sugar mixtures present in plant biomass hydrolysates have been very promising even though the reported success with regard to the utilization of L-arabinose still lags behind that of D-xylose (Cunha et al., 2019; Francois et al., 2020; Kwak and Jin, 2017; Wang et al., 2019; Ye et al., 2019). In addition to broadening substrate utilization, numerous efforts in engineering the popular cell factory for the production of value-added products other than ethanol have been reported with a few processes already being commercialized (Borodina and Nielsen, 2014; Hong and Nielsen, 2012; Nevoigt, 2008).

D-GalUA is more oxidized than neutral sugars and several microbial

pathways exist for its catabolism (Richard and Hilditch, 2009). The establishment of D-GalUA utilization in *S. cerevisiae* has been the focus of several previous studies. It has not been possible to express all enzymes of a bacterial pathway in their active form (Huisjes et al., 2012b). However, the heterologous expression of enzymes constituting a fungal pathway resulted in marginal D-GalUA consumption (Biz et al., 2016; Jeong et al., 2020; Protzko et al., 2018). The latter pathway seems conserved among fungi able to metabolize D-GalUA (Chroumpi et al., 2020; Protzko et al., 2019). As illustrated in Fig. 1b, the carbon enters the central metabolism via pyruvate and glycerol and two enzymatic steps require reducing equivalents in the form of NAD(P)H (Hilditch et al., 2007). Without the addition of an electron-donating co-substrate, D-GalUA catabolism via the fungal pathway seems to be inefficient. In fact, wild-type *A. niger* was only able to produce biomass very slowly in minimal medium with D-GalUA as the sole source of carbon and energy (Alazi et al., 2017). By using ^{13}C labelled D-GalUA, marginal consumption of this substrate in complex medium was proven in an engineered *S. cerevisiae* strain equipped with the fungal pathway by Biz et al. (2016) who used fructose as co-substrate. Protzko et al. (2018) optimized the D-GalUA pathway in *S. cerevisiae* and claimed slow utilization of D-GalUA in synthetic medium containing amino acids without an additional co-substrate. Jeong et al. (2020) used an engineered strain equipped with pathways for L-arabinose, D-xylose and D-GalUA utilization. Based on the reported volumetric rate achieved in the presence of these three carbon sources in complex medium ($0.49 \, g \, L^{-1} \, h^{-1}$) and the value for the initial biomass concentration ($25 \, g_{CDW} \, L^{-1}$), one can conclude the specific rate of D-GalUA consumption did not exceed a value of $0.02 \, g \, g_{CDW}^{-1} \, h^{-1}$. Thus, none of the previously reported capabilities of *S. cerevisiae* to metabolize D-GalUA has been industrially relevant.

One reason for the low efficiency has been assumed to result from the fact that the constructed *S. cerevisiae* strains were barely able to channel glycerol, one of the products of the fungal D-GalUA catabolic pathway (Fig. 1b), into the yeast's central carbon catabolism. In fact, two of the three *S. cerevisiae* strains used in the above-mentioned studies (Biz et al., 2016; Protzko et al., 2018) are definitely known to either grow slowly or not at all in synthetic glycerol medium without amino acids and nucleic bases (Swinnen et al., 2013). Apart from this, switching metabolism of D-GalUA from respiration to fermentation has remained another unsolved challenge. It is unclear whether D-GalUA can support alcoholic fermentation under aerobic conditions by overflow metabolism and carbon catabolite repression, i.e. characteristics well-known for the species *S. cerevisiae* when it grows in D-glucose or other hexose sugars (Hagman and Piškur, 2015). Moreover, the anaerobic conversion of D-GalUA to ethanol is in principle impossible due to the substrate's insufficient degree of reduction. The use of a co-substrate that is more reduced than neutral sugars could provide a solution to the redox problem. In this respect, glycerol could serve as an ideal co-substrate, since not only does it have a higher degree of reduction (da Silva et al., 2009; Wendisch et al., 2011; Yazdani and Gonzalez, 2007), but can deliver exactly the number of electrons required for redox homeostasis during fermentation of D-GalUA to ethanol. In fact, anaerobic co-fermentation of D-GalUA and glycerol to ethanol would allow the same redox balance as in the conversion of D-glucose to ethanol. One mol D-GalUA and 2 mol glycerol can theoretically be converted by anaerobic fermentation into 4 mol ethanol and 4 mol CO_2 providing both a carbon and electron balance (Supplementary Fig. 1; Supplementary Eqs. (1)-(3)).

Glycerol is a major by-product of several industries, most notably biodiesel production and fermentation of alcoholic beverages. In 2018 alone, the oleochemical market had a glycerol output of 2.8 million tonnes, bringing a sharp drop in crude glycerol prices. This resulted in crude glycerol being on the verge of becoming a waste stream rather than a commodity (Russmayer et al., 2019). In contrast to pure glycerol, the glycerol resulting from biodiesel production (commonly known as 'crude glycerol') contains high levels of contaminants, in particular methanol, soap and salts, presenting an additional challenge for its
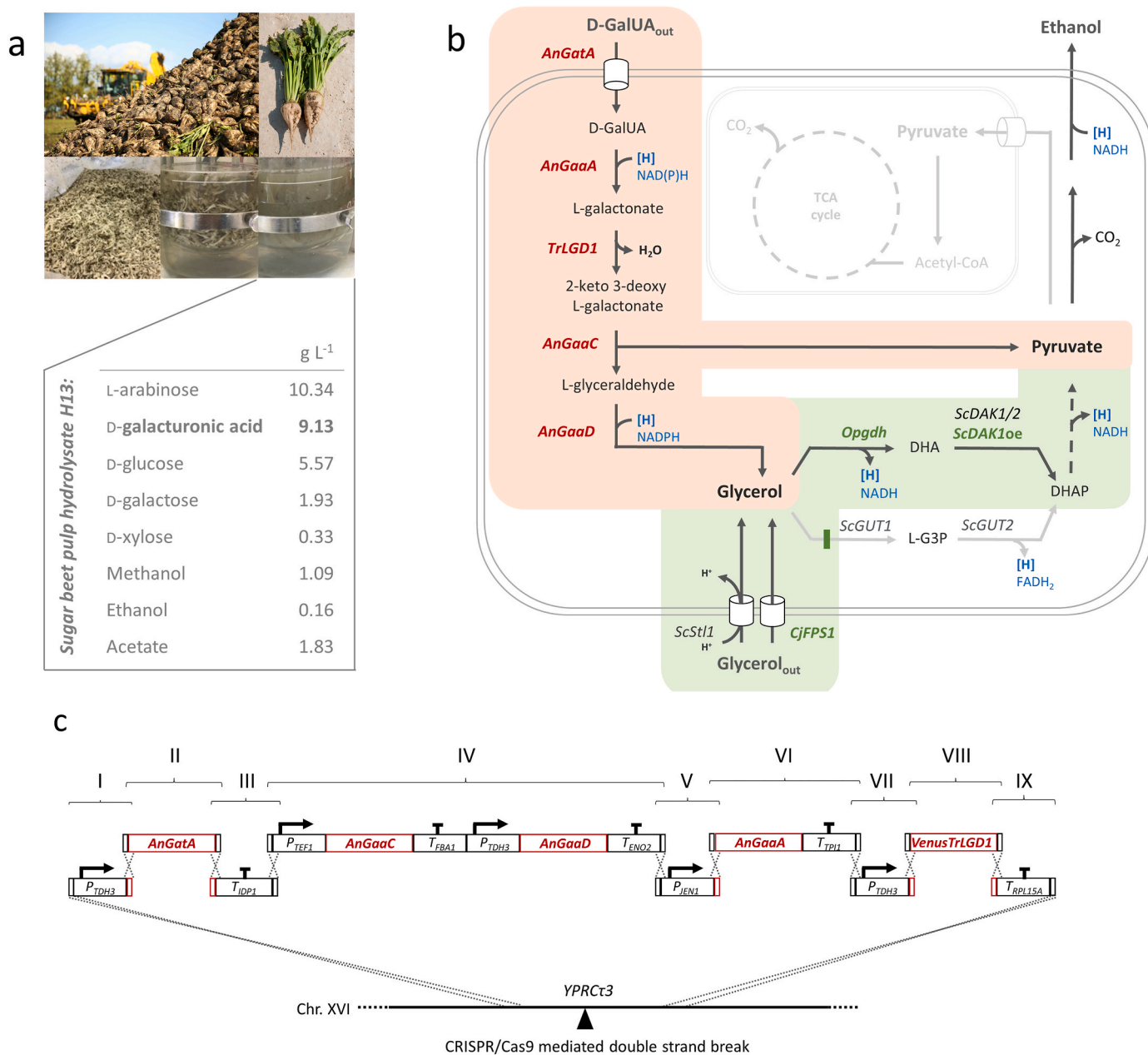
Fig. 1. Engineering of *S. cerevisiae* for the co-utilization of D-galacturonic acid (D-GalUA) and glycerol. **a** Sugar beet pulp (left over after industrial sugar extraction) is a biomass residue rich in pectin. Enzymatic hydrolysis releases a mixture of carbon sources among which D-GalUA is a major constituent. The composition of one representative hydrolysate generated in this study (H13) is shown. **b** Concept of co-utilizing D-GalUA and glycerol (a by-product from biodiesel production industry) by engineered *S. cerevisiae* equipped with a fungal pathway for the utilization of D-GalUA (in red) and a modified glycerol catabolism (in light green). Feeding of extracellular glycerol provides additional electrons from glycerol oxidation in the form of NADH. **c** Implementation of nine repair fragments to establish the expression cassettes comprising the fungal D-GalUA pathway by means of CRISPR/Cas9 in the reference strain Gly (able to utilize glycerol efficiently via an NAD-dependent pathway) to obtain the strain Gly/GalUA. Genes for D-GalUA utilization were derived from either *Aspergillus niger* (*An*) or *Trichoderma reesei* (*Tr*). Improved glycerol utilization was achieved by modifications of endogenous *Saccharomyces cerevisiae* (*Sc*) genes and the implementation of heterologous genes from *Cyberlindnera jadinii* (*Cj*) and *Ogataea parapolymorpha* (*Op*). AnGatA: D-GalUA transporter, AnGaaA: NAD(P)-dependent D-GalUA reductase, VenusTrLGD1: L-galactonate dehydratase fused to the *Venus* yellow fluorescent protein tag, AnGaaC: 2-keto 3-deoxy L-galactonate aldolase, AnGaaD: NADP-dependent L-glyceraldehyde reductase, ScSTL1: glycerol/H$^+$ symporter, CjFPS1: aquaglyceroporin ('glycerol facilitator'), Opgdh: NAD-dependent glycerol dehydrogenase, ScDAK1/2: dihydroxyacetone kinases (ScDAK1oe: overexpression of ScDAK1), ScGUT1: glycerol kinase, ScGUT2: mitochondrial FAD-dependent L-glycerol 3-phosphate dehydrogenase.

industrial valorization (Kumar et al., 2019; Yang et al., 2012). Nevertheless, the successful utilization of crude glycerol as a carbon source in industrially relevant biotechnological processes is state of the art (Li et al., 2018; Russmayer et al., 2019) and despite the presence of growth-inhibitory compounds, yeasts are generally robust towards the concentrations found in this substrate (Taccari et al., 2012).

The improvement of *S. cerevisiae*'s capacity to channel glycerol into

the central carbon catabolism has been a major achievement of previous work in our laboratory (Ho et al., 2017, 2018; Klein et al., 2016a, 2016b; Swinnen et al., 2016). The resulting knowledge has been a great asset to embark on co-fermentation of D-GalUA and glycerol, particularly since we were already able to channel carbon from glycerol, previously considered a 'non-fermentable' substrate in *S. cerevisiae,* to the generation of fermentation products such as 1,2-propanediol (Islam et al.,

2017) and ethanol (Aβkamp et al., 2019). Significant ethanol formation from glycerol was particularly obtained when oxygen availability was reduced by increasing the filling volume in aerobic shake flasks (Aβkamp et al., 2019). Essential genetic modifications to achieve this were the replacement of the endogenous FAD-dependent glycerol catabolic pathway (L-glycerol 3-phosphate pathway) by the so-called 'dihydroxyacetone (DHA) pathway' and the expression of a heterologous aquaglyceroporin, e.g. Fps1 from *Cyberlindnera jadinii* (Fig. 1b). Unlike the endogenous Stl1-mediated uptake mechanism that involves translocation of protons across the membrane, the alternative Fps1-route has been assumed to occur via a channel-like glycerol uptake that does not require net ATP. In addition, the DHA pathway saves all electrons from glycerol in the form of cytosolic NADH which is assumed to facilitate fermentative metabolism of glycerol. Interestingly, the respective genetic modifications also improved the growth rate on glycerol.

A yeast strain engineered with a DHA pathway/aquaglyceroporin for glycerol utilization has been assumed to be able to i) better connect the fungal D-GalUA pathway with the central carbon metabolism and ii) allow the supply of extra reducing power by co-feeding glycerol (Fig. 1b). Thus, such a strain appeared to be a highly promising starting point for the endeavor of the current study to approach D-GalUA/glycerol co-utilization and even co-fermentation. Here, five heterologous expression cassettes comprising the fungal pathway for D-GalUA catabolism were designed by using strong 'glycerol-active' promoters and incorporated together in a single genomic location previously reported to result in high expression levels. This study represents an important milestone towards the long-term goal of pectinolytic-waste valorization by delivering a strain capable of a high specific D-GalUA consumption rate and a proof of concept for co-fermentation of D-GalUA and glycerol to ethanol.

2. Results

2.1. Engineering S. cerevisiae for D-GalUA/glycerol co-utilization

A 'DHA pathway strain' of *S. cerevisiae* constructed before (Ho et al., 2018) served as a baseline strain. It is a derivative of the popular laboratory strain *S. cerevisiae* CEN.PK113-1A in which the native *UBR2* allele has been replaced by the respective allele from strain CBS 6412-13A, a genetic modification crucial for establishing growth of CEN.PK strains in synthetic glycerol medium (Swinnen et al., 2016). Moreover, this strain carries the 'DHA pathway' for glycerol catabolism as well as a heterologous aquaglyceroporin (Fps1 ortholog) as depicted in Fig. 1b. In the respective study, Ho et al. (2018) tested different glycerol-active promoters to control the overexpression of *DAK1* (encoding a dihydroxyacetone kinase isoenzyme in *S. cerevisiae*) and the strain with the strong *ADH2* promoter showed the highest growth rate (0.24 h^{-1}) in synthetic glycerol medium. This strain, referred to here as the Gly reference strain, was used to establish a fungal reductive pathway for D-GalUA catabolism (Fig. 1b). The individual fungal enzymes used in the current work have been shown to be active in *S. cerevisiae* in previous studies. However, here we selected a novel combination of the hitherto best-performing enzymes with the goal of improving the overall performance of the pathway. These enzymes are the D-GalUA reductase (GaaA) and L-glyceraldehyde reductase (GaaD) from *A. niger* (Biz et al., 2016) and the *A. niger* D-GalUA transporter (GatA), the yellow fluorescent protein-fused *T. reesei* L-galactonate dehydratase (Venus-LGD1) and the *A. niger* 2-keto 3-deoxy L-galactonate aldolase (GaaC) (Protzko et al., 2018). The activity of the L-galactonate dehydratase has been previously considered rate-controlling for the D-GalUA catabolic pathway initially expressed in *S. cerevisiae* by Biz et al. (2016). Fusing the open reading frame of the *T. reesei* LGD1 to the Venus tag has been demonstrated by Protzko et al. (2018) to result in a 60-fold increase in specific *in vitro* enzyme activity.

The predominant goal of the current study was to deliver a proof of concept for a co-fermentation of two carbon sources that are naturally respired in fungi. Therefore, we wanted to ensure high expression levels of the five fungal coding sequences in non-fermentable carbon sources and used promoters that are particularly strong in glycerol medium (Ho et al., 2018). Moreover, the unique combinations of promoters and terminators were meant to prevent excision of the assembled parts by homologous recombination. Details about the constructed expression cassettes and their site of integration (Flagfeldt et al., 2009) are shown in Fig. 1c. The resulting strain created for the co-consumption of D-GalUA and glycerol is referred to here as the Gly/GalUA strain. It should be noted that GaaA prefers NADPH as a cofactor (but can also use NADH), and GaaD is assumed to exclusively use NADPH (Fig. 1b) (Martens-Uzunova and Schaap, 2008).

2.2. Efficient D-GalUA consumption by the strain Gly/GalUA requires a co-substrate

It is generally accepted that certain filamentous fungi bearing the common reductive D-GalUA catabolic pathway are able to utilize this uronic acid as the sole source of carbon in minimal medium even though with very low rates as mentioned in the introduction. Our constructed Gly/GalUA strain was equipped with enzymes/transporter from the filamentous fungi *A. niger* and *T. reseei* for D-GalUA metabolism and was optimized for glycerol utilization. The latter is considered to be relevant since glycerol is one of the end-products of the fungal D-GalUA pathway. From a fundamental point of view, it was interesting to check whether our strain can aerobically utilize D-GalUA as the sole source of carbon and energy in defined synthetic medium (SM_{Gly}) even without the addition of growth supplements such as nucleic bases or amino acids. As we assumed that D-GalUA catabolism requires a fully respiratory metabolism, we chose a 10% filling volume commonly used for aerobic shake flask cultivations. The Gly/GalUA strain indeed seems to have consumed about 1.6 g L^{-1} in 48 h under these conditions even without a co-substrate (Fig. 2). Moreover, the detected D-GalUA 'consumption' can be linked to the implemented D-GalUA transporter/pathway since the decrease in D-GalUA was not detected when the Gly reference strain was cultivated under the same conditions (Fig. 2). Still, there was no biomass formation at all and the data are not sufficient to dissect whether D-GalUA indeed ended up in the central carbon catabolism, accumulated inside the cells or was converted to another compound via a simple biotransformation.

Next, we checked the effect of adding glycerol as an electron-donating co-substrate on D-GalUA catabolism in synthetic medium. Indeed, about 5 g L^{-1} D-GalUA was utilized in less than 24 h in the presence of glycerol (Fig. 2). The results demonstrate for the first time that glycerol can serve as an efficient co-substrate for D-GalUA utilization when using a *S. cerevisiae* strain with a modified glycerol catabolism.

An interesting auxiliary result of the experiments shown in Fig. 2 was that the Gly reference strain also seemed to take up about 1.4 g L^{-1} D-GalUA in the presence of glycerol especially at a later phase of cultivation. The results obtained with the Gly reference strain seem to be consistent with previous findings that i) some D-GalUA can be taken up by one or more endogenous uptake mechanism(s) in *S. cerevisiae* (Protzko et al., 2018; Souffriau et al., 2012) and ii) one or more endogenous reductase(s) in *S. cerevisiae* can convert D-GalUA to L-galactonate (L-GalA), the first intermediate of the D-GalUA pathway (Benz et al., 2014).

2.3. A maximum specific D-GalUA consumption rate of 0.23 g $g_{CDW}^{-1} h^{-1}$ was achieved

Despite glycerol being considered a purely respiratory carbon source in wild-type *S. cerevisiae* (Klein et al., 2017), we knew that DHA pathway strains of *S. cerevisiae* produce ethanol from glycerol as the sole carbon source, when the maximum oxygen transfer rates were reduced by increasing the filling volume of the employed shake flasks (Aβkamp
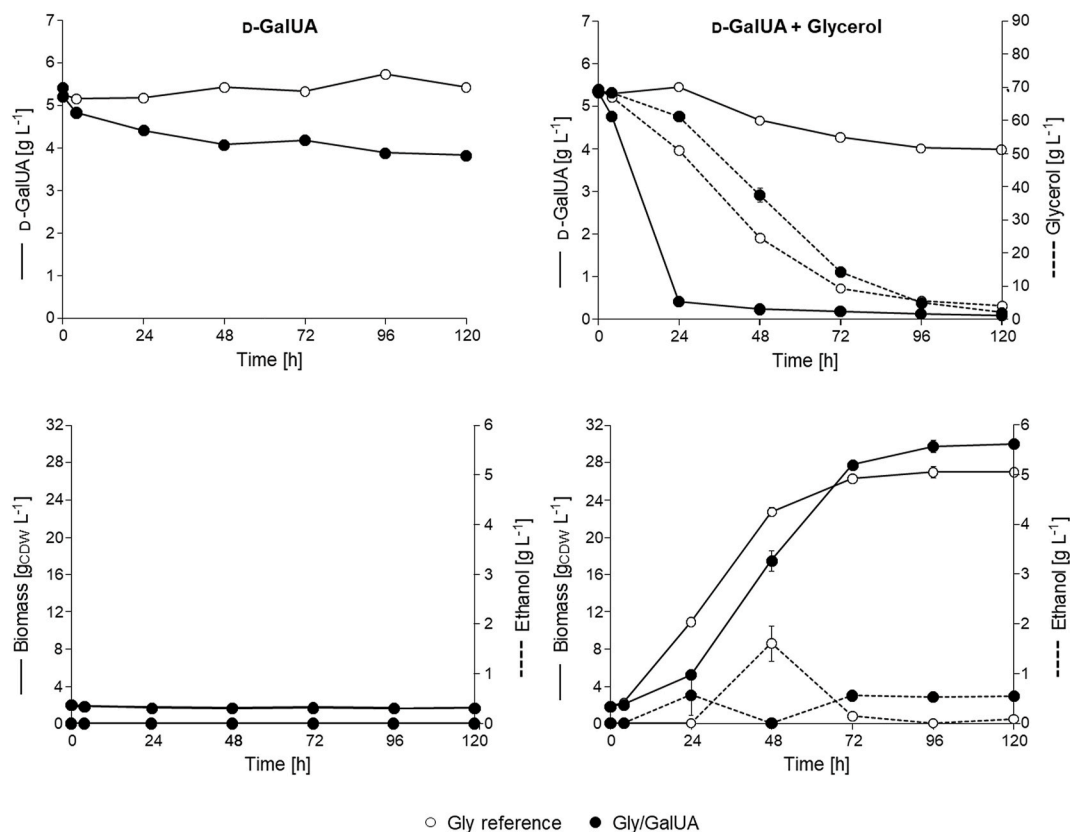
Fig. 2. Aerobic shake flask cultivations (10% filling volume) with the *S. cerevisiae* strain Gly/GalUA equipped with the fungal reductive pathway for D-galacturonic acid (D-GalUA) utilization and the corresponding baseline strain with a modified glycerol catabolism (Gly reference). Experiments were carried out in $SM_{D-GalUA}$ with and without glycerol at initial pH 5. Cells pre-grown in SM_{Glu} were washed, inoculated at initial cell density of 1.7 g_{CDW} L^{-1} (corresponding to an OD_{600} of about 4) in flasks filled at 10% of their maximum filling volume and incubated at 200 rpm. Average values and standard deviations from three biological replicates are shown.

et al., 2019). Ethanol formation from glycerol is not redox-neutral, resulting in a surplus of electrons (Supplementary Eq. (2)). With the experiment shown in Fig. 3, we tested whether the catabolism of D-GalUA, despite being a respiratory carbon source in fungi, can serve as an electron sink and increases ethanol yield from glycerol in our strain Gly/GalUA. We used the same experimental setup as reported by Aβkamp et al. (2019) using 20% filling volume and the relatively high glycerol concentration (75 g L^{-1}) that has been standard in our laboratory.

Without the addition of D-GalUA, both strains showed a maximum ethanol titer between 4 and 5 g L^{-1}. Despite expectations, the addition of D-GalUA under these cultivation conditions did not increase ethanol titer, but significantly reduced it in the strain that carries the fungal D-GalUA pathway. A closer look at the biomass production shows that it was delayed for this strain in the presence of D-GalUA, indicating a negative impact of D-GalUA uptake and/or metabolism on growth. The decreased initial biomass formation could have resulted in a slower depletion of dissolved oxygen and thus a delayed switch to respiro-fermentative metabolism. Moreover, it cannot be excluded that the mass flow through particular biochemical reactions and *in vivo* enzyme activities might have changed by the transport and metabolism of D-GalUA. In fact, nothing is known so far about the effect of D-GalUA on the central metabolism of *S. cerevisiae*.

Although the expected supportive effect of D-GalUA addition on ethanol production could not be demonstrated in the experiment shown in Fig. 3, it verified the impressive capability of the Gly/GalUA strain to consume D-GalUA in the presence of glycerol. Although the initial biomass concentration was only 0.09 g_{CDW} L^{-1} in this experiment (Fig. 3), a volumetric consumption rate of 0.256 ± 0.029 g L^{-1} h^{-1} was obtained. An estimation of the maximum specific D-GalUA consumption

rate resulted in a value of 0.226 ± 0.006 g g_{CDW}^{-1} h^{-1} (Supplementary Table 1).

2.4. Ethanol formation from co-fermentation of D-GalUA and glycerol

The negative impact of D-GalUA on growth of the Gly/GalUA strain obviously hampered the co-fermentation of D-GalUA and glycerol to ethanol in the previous experiment (Fig. 3). Therefore, we changed the experimental conditions by i) increasing the initial cell density (which also facilitated reaching oxygen-limited conditions), ii) pulsing the D-GalUA under conditions where ethanol formation from glycerol alone was observed and iii) increasing the D-GalUA concentration. When SM_{Gly} medium was inoculated with 1.7 g_{CDW} L^{-1}, ethanol started to be formed from glycerol alone after about 24 h. At this point in time, i.e. when the biomass concentration had reached a value of 7.7 g_{CDW} L^{-1}, D-GalUA was pulsed at a final concentration of 12 g L^{-1}. Notably, the latter D-GalUA concentration reflects the concentration present in our sugar beet pulp hydrolysate (Fig. 1a). Another reason for increasing D-GalUA concentration was our concern to obtain a significant difference between the amount of ethanol formed from glycerol plus D-GalUA versus glycerol alone. The control experiment was conducted under identical conditions with the same volume (2.5 mL) of water spiked to the glycerol-utilizing cells. Compared to the addition of water, the addition of D-GalUA under these conditions resulted in a significantly faster accumulation of ethanol (Fig. 4). After 8 h of consuming the added D-GalUA, an ethanol titer of 4.4 ± 0.2 g L^{-1} was detectable. In contrast, the ethanol titer at this time point under the control conditions (water addition) was only 1.3 ± 0.3 g L^{-1}. Biomass formation and the uptake of external glycerol were virtually the same in the water control and the D-GalUA pulse experiment. A control experiment was conducted also
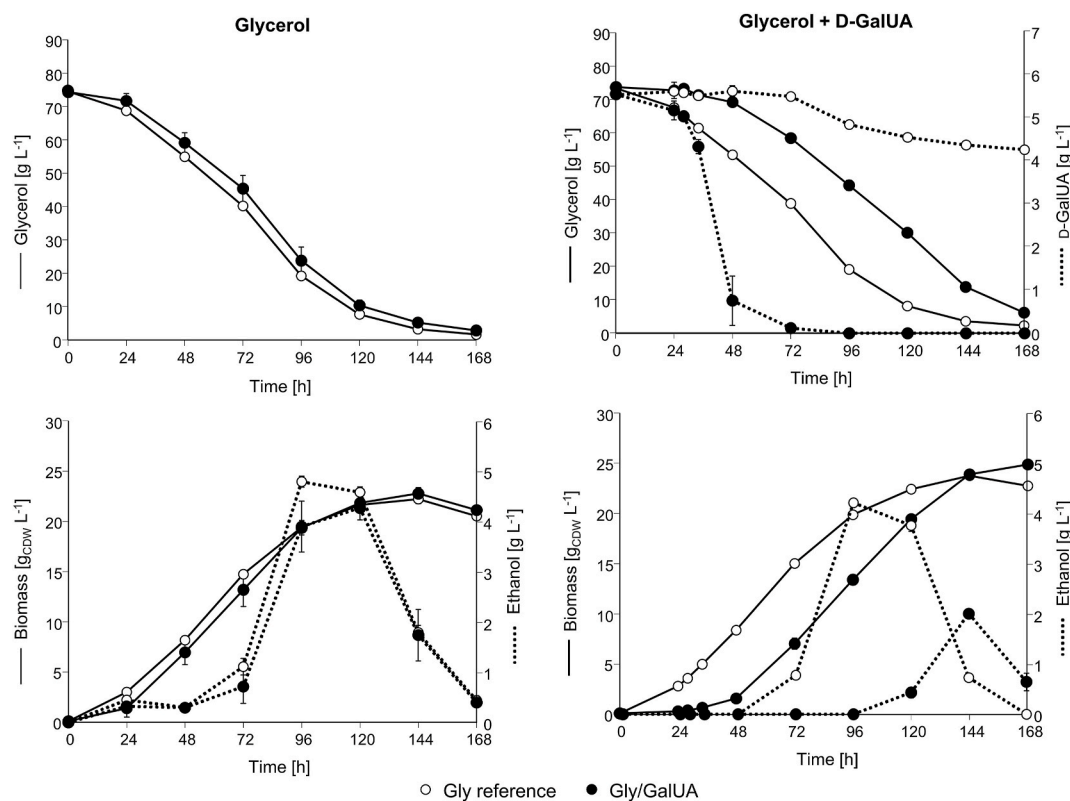
Fig. 3. Consumption of D-GalUA and glycerol as well as formation of biomass and ethanol by the *S. cerevisiae* baseline strain (Gly reference utilizing glycerol via the aquaglyceroporin/DHA pathway) and the corresponding strain Gly/GalUA additionally equipped with the fungal reductive pathway for D-galacturonic acid (D-GalUA) utilization. Cells were pre-grown in SM_{Glu}, washed, and used to inoculate SM_{Gly} medium (initial pH of 5 and supplemented with D-GalUA as indicated) with a biomass density of 0.09 g_{CDW} L^{-1} (corresponding to an OD_{600} of about 0.2). Shake flasks (20% filling volume) were incubated at 200 rpm. Average values and standard deviations from four biological replicates are shown.

based on a D-GalUA pulse but using the Gly reference strain (Supplementary Fig. 2). It showed that a strain not engineered for efficient D-GalUA utilization cannot produce ethanol when the uronic acid is pulsed. This result excludes that the mere presence of the weak acid D-GalUA at the tested concentration and in the reference strain caused by itself any switch of metabolism towards ethanol formation. The oxygen availability was obviously low enough to reduce respiratory capacity sufficiently to favor alcoholic fermentation. Still, ethanol seemed to be slowly consumed in a later phase of the cultivation indicating that the oxygen transfer into the culture was still sufficient to support ethanol metabolization.

As a next step, it was of interest to test the Gly/GalUA strain under oxygenation levels that represent industrially relevant conditions. For this purpose, the spiking experiment was repeated in a different set-up by sealing the flasks with airlocks directly after D-GalUA addition. The airlocks allowed the release of carbon dioxide but prevented additional oxygen intake throughout the fermentation. However, virtually no additional biomass accumulation or glycerol consumption was observed under these conditions (Supplementary Fig. 3). A minimal amount (0.54 g L^{-1}) of uronic acid was removed from the medium by the Gly/GalUA strain that contains the D-GalUA pathway. This amount was slightly higher when compared with the Gly reference strain under the same conditions and a slightly higher formation of ethanol was detected even though the absolute values were marginal.

We also checked the performance of our strain under conditions in which the oxygen availability was reduced but the reduction was supposed to be less severe compared to the use of air-locks. For this purpose, a relatively high initial biomass density (4.7 g_{CDW} L^{-1}) was used. In the respective experiment, D-GalUA was added from the beginning in order to test whether this scenario could also result in significant ethanol formation as soon as the D-GalUA concentration is high which is in

contrast to the experiment shown in Figs. 2 and 3. The results in Fig. 5 clearly show that the strain Gly/GalUA, under these conditions, formed ethanol not only significantly faster, but reached a much higher titer compared to the Gly reference strain (6.8 ± 0.2 g L^{-1} vs 0.8 ± 0.5 g L^{-1} after 19 h). The highest ethanol yields were achieved at the beginning of the D-GalUA consumption phase. The maximum yield that was obtained (at the basis of reliable ethanol titers) was 0.48 ± 0.06 C-mol C-mol$_{substrates (D-GalUA+glycerol)}^{-1}$ was calculated after 7 h of cultivation. This accounts for approximately 71% of the maximum theoretical yield for the co-fermentation of 2 mol glycerol and 1 mol D-GalUA which corresponds to 0.67 C-mol$_{ethanol}$ per C-mol$_{substrates}$ (Supplementary Eq. (3), Supplementary Fig. 1). The overall product yield of the first 19 h time period (D-GalUA was depleted at about 19 h) was 0.34 ± 0.01 C-mol$_{E-thanol}$ per C-mol$_{substrates}$ which is 50.5% of the maximum theoretical yield. The ethanol yield declined over time, dropping significantly after D-GalUA was consumed,. After 48 h (i.e. when the maximum ethanol titer was achieved), the yield was reduced to 0.30 ± 0.01 C-mol$_{ethanol}$ per C-mol$_{substrates}$.

2.5. ^{13}C labelling and intracellular pyruvate measurements confirmed co-fermentation of D-GalUA and glycerol to ethanol

The results shown in Figs. 4 and 5 strongly suggest that a co-fermentation of D-GalUA and glycerol is actually occurring in our Gly/GalUA strain. However, one could argue that addition of D-GalUA might have simply caused a metabolic shift in the strain Gly/GalUA as a response to acid stress. In order to unambiguously prove that the ethanol was indeed formed from both carbon sources and not only from glycerol, ^{13}C tracing was realized in strain Gly/GalUA by using labelled [U–$^{13}C_3$]-glycerol. The decision for using labelled glycerol (instead of labelled D-GalUA) was driven by cost effectiveness. For the same reason, we
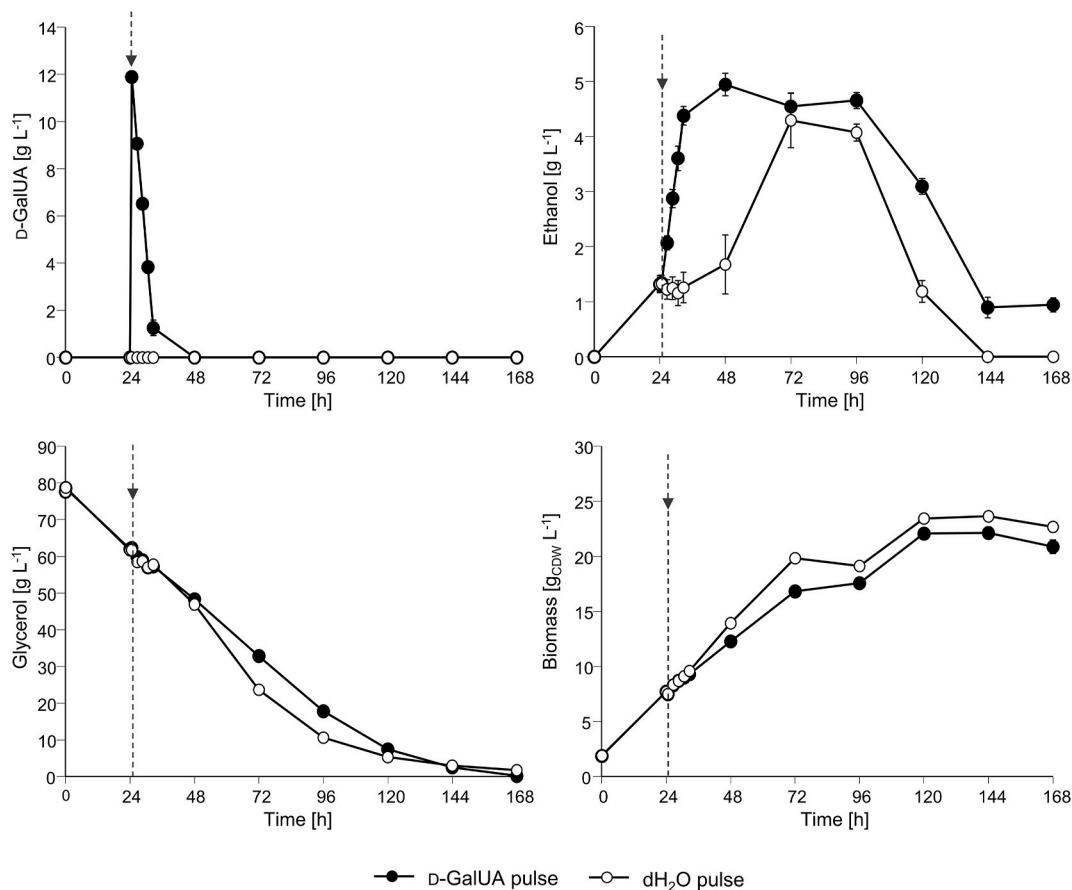
Fig. 4. Effect of pulsing D-GalUA to a glycerol-utilizing culture of the *S. cerevisiae* strain Gly/GalUA on glycerol consumption as well as the formation of ethanol and biomass. The 24 h sample was the last sample taken before the pulse. The biomass density at this time point was about 7.7 g_{CDW} L^{-1}. The D-GalUA pulse (by adding 2.5 mL of a concentrated D-GalUA solution) was realized at 24.7 h (red arrow), when the strain already started to form ethanol from glycerol alone. In a control experiment, the same volume of deionized water (dH$_2$O) was added. Cells were incubated at 200 rpm. Average values and standard deviations of biological quadruplicates are shown.

reduced the initial glycerol concentration to 25 g L^{-1} even though this resulted in a lower ethanol titer (Supplementary Fig. 4). Before addition of labelled glycerol and non-labelled D-GalUA, the cells were pre-grown in [U–^{12}C$_3$]-glycerol and carefully washed to ensure the removal of any non-labelled glycerol. Labelling patterns in pyruvate are the consequence of labelled glycerol uptake and served as a proxy for ethanol labelling (Supplementary Fig. 5). The latter was analytically not accessible. The percentage of labelled intracellular pyruvate was significantly reduced in the presence of D-GalUA (Fig. 6a). As the increased portion of non-labelled pyruvate must have resulted from D-GalUA metabolism, the results confirm the glycerol/D-GalUA co-fermentation.

Using biomass samples of the [U–^{13}C$_3$]-glycerol experiment (Supplementary Fig. 4), we also determined the dynamics of the total intracellular pyruvate pools of cells growing in the presence and absence of D-GalUA. D-GalUA consumption clearly led to a strong accumulation of pyruvate, which was not visible in the control experiment with glycerol as the sole source of carbon (Fig. 6b).

2.6. Aerobic co-consumption of D-GalUA and glycerol in a defined medium containing a mixture of metabolizable carbon sources mimicking the composition of SBP hydrolysate

Although the Gly/GalUA strain obviously requires further genetic modifications for more efficient ethanol production (see discussion), it utilized D-GalUA in a relatively efficient manner compared to previous reports (Biz et al., 2016; Jeong et al., 2020; Protzko et al., 2018). It was therefore of interest to check the performance of substrate consumption

in a mixture of carbon sources. In fact, hydrolysates of pectin-rich biomass represent mixtures of fermentable and non-fermentable carbon sources. We generated a hydrolysate of SBP by treating the latter with a mix of commercial enzymes, Viscozyme L and Celluclast (see Methods). This treatment resulted in a high degree of saccharification. About 30% of the SBP hydrolysate was D-GalUA; the concentrations of the detected carbon sources are depicted in Fig. 1a.

A fundamental question arose regarding the extent to which the other carbon sources present in the concentrations obtained in SBP hydrolysate (Fig. 1a) can also support D-GalUA consumption under aerobic conditions. A YNB-based defined medium was prepared that contained similar concentrations of D-glucose, L-arabinose, D-GalUA, D-galactose and acetic acid as the SBP hydrolysate H13 shown in Fig. 1a. The pH was adjusted to 5 and the medium is referred to here as "synthetic hydrolysate" (Fig. 1a). The experiment revealed that the other carbon sources indeed support D-GalUA utilization. However, only about half of the D-GalUA was consumed without glycerol, while the addition of glycerol allowed the complete consumption of the 9 g L^{-1} D-GalUA. As expected, D-glucose was consumed first and rapidly (Fig. 7). It seems that the major part of D-GalUA was used in parallel with D-galactose, and the non-fermentable carbon sources such as acetic acid and/or ethanol. It can be concluded that the other carbon sources alone, at least at their concentrations present in our SBP hydrolysate do not allow the complete consumption of the D-GalUA present.
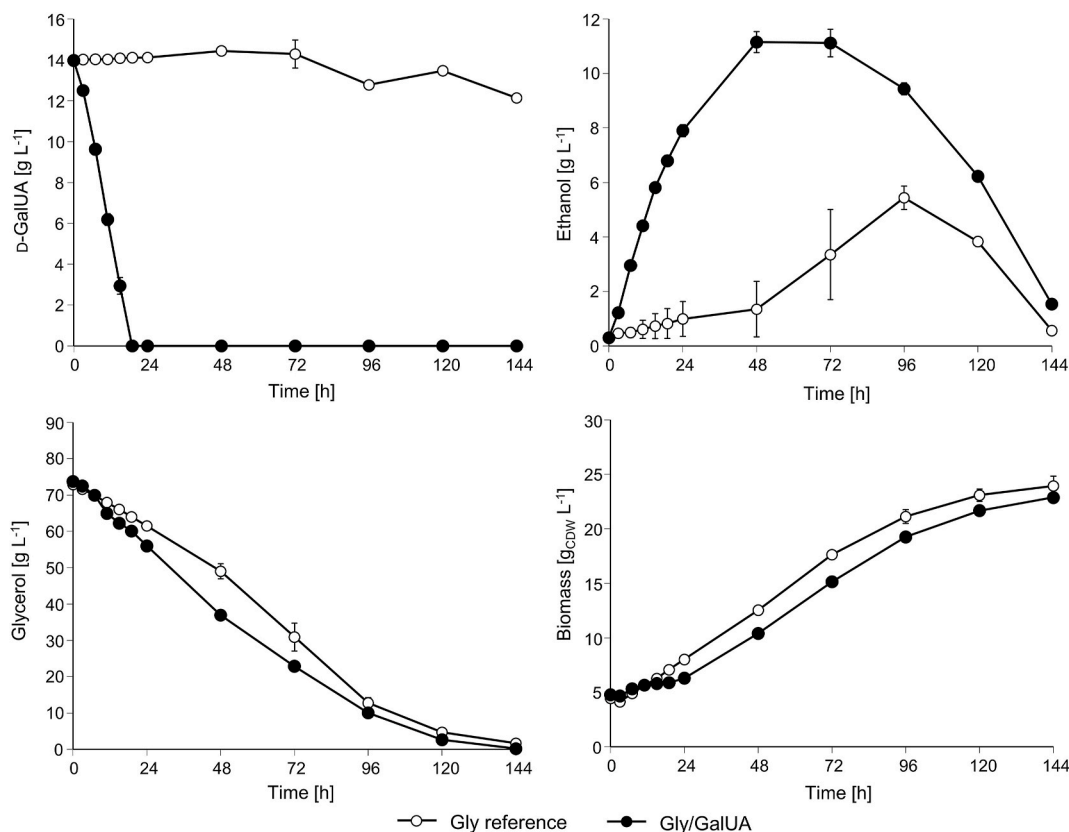
Fig. 5. High cell density batch shake flask cultivations with the *S. cerevisiae* strain Gly/GalUA and the Gly reference strain in SM_{Gly} supplemented with 1.4% (w v^{-1}) D-GalUA at an initial pH 5 and inoculated at a cell density of 4.7 g_{CDW} L^{-1}. Cells were pre-grown in SM_{Gly} (to obtain sufficient biomass and pre-adapt the cells to growth on glycerol). The main cultures were incubated at 200 rpm. The experiment was performed in biological duplicates. Average values and mean absolute deviations are shown.
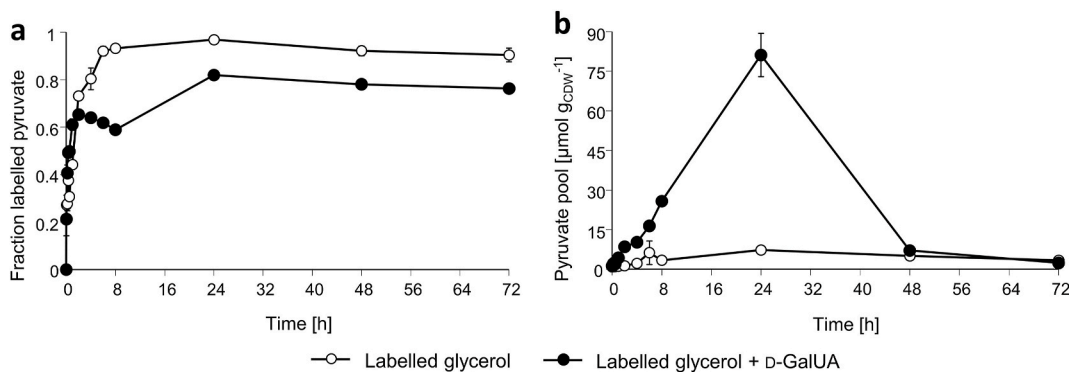

Fig. 6. Total fraction of ^{13}C-labelled intracellular pyruvate **(a)** and total intracellular pyruvate accumulation **(b)** in a cultivation of the strain Gly/GalUA with and without D-GalUA addition in SM_{Gly} medium containing 30 g L^{-1} [U–$^{13}C_3$]-labelled glycerol instead of [U–$^{12}C_3$]-glycerol. Pyruvate labelling is used as a proxy for ethanol labelling. Labelled glycerol and unlabelled D-GalUA were added at t = 0 h. Mean values and standard deviations of biological triplicates are shown. The time courses for the concentration of extracellular glycerol, D-GalUA, biomass and ethanol are shown in Supplementary Fig. 4. More detailed information regarding the ^{13}C labelling experiment can be extracted from Supplementary Fig. 5.

### 2.7. D-GalUA can be efficiently consumed in glycerol-supplemented SBP hydrolysate

After demonstrating D-GalUA consumption of our strain in synthetic hydrolysate, the strain was also tested in crude SBP hydrolysate supplemented with glycerol and enriched with YNB. As the presence of acetic acid did not seem to have a major impact at an initial pH 5 in the synthetic hydrolysate, we tested lower pH values (3.5 and 4.5) in the crude hydrolysate. In fact, the toxic effect of weak acids such as acetic acid and D-GalUA is known to strongly increase at pH values around and

below their pK$_a$ (4.75 and 3.51, respectively). At pH 3.5, biomass formation and the consumption of all carbon sources was indeed severely compromised. The consumption of D-GalUA and glycerol appeared to be affected most. However, the metabolization of all carbon sources, including D-GalUA, was fairly efficient in crude hydrolysate at an initial of pH 4.5 even though this pH is below the pK$_a$ of acetic acid (4.75). Similar to the results in synthetic hydrolysate, the relatively small amount of D-glucose was consumed first accompanied by some ethanol formation (Fig. 8). After this phase, there was a rapid decline in D-GalUA concentration. The maximum specific D-GalUA consumption rate in the
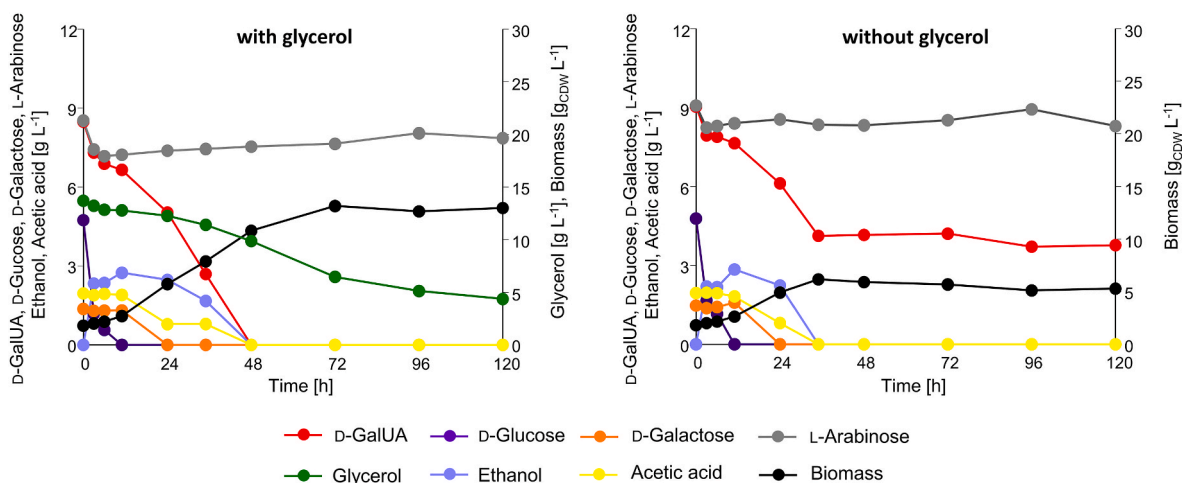
Fig. 7. Aerobic shake flask cultivations with the *S. cerevisiae* strain Gly/GalUA in a defined medium mimicking the composition of sugar beet pulp (SBP) hydrolysate with and without the addition of glycerol. This medium is referred to as 'synthetic SBP hydrolysate' and contains YNB_{waa} and a mixture of the main carbon sources generally present in SBP hydrolysates such as D-glucose, D-galactose, L-arabinose, D-GalUA and acetic acid. Cells were pre-grown in $YNB_{w/oaaGlu}$, inoculated at initial cell density of 1.82 g_{CDW} L^{-1} and incubated at 250 rpm.
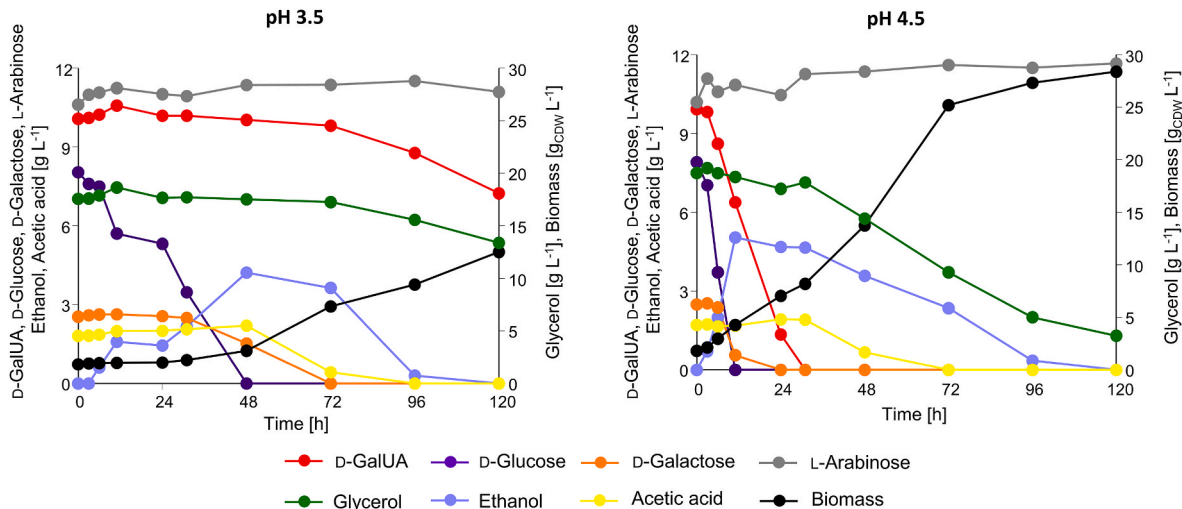
Fig. 8. Batch shake flask cultivations with the *S. cerevisiae* strain Gly/GalUA in crude SBP hydrolysate (endogenously containing 30 mM acetic acid) at initial pH of 4.5 and 3.5. The SBP hydrolysate was enriched with YNB_{waa}. Cells were pre-grown in YNB_{Glu}, inoculated at initial cell density of 1.82 g_{CDW} L^{-1} and incubated at 250 rpm.

crude medium was 0.123 g g_{CDW}^{-1} h^{-1} (Supplementary Table 1).

We also tested the strain Gly/GalUA in SBP hydrolysate in the presence of crude glycerol at a concentration of about 50 g L^{-1} (Supplementary Fig. 6). The experimental conditions were different from those used in the experiments shown in Fig. 8. However, the results show that D-GalUA was completely used as well. The calculated D-GalUA consumption rate in this experiment was 0.076 ± 0.001 g g_{CDW} h^{-1} (Supplementary Table 1). Although we do not have a direct comparison to pure glycerol (tested under exactly the same conditions), the negative effect of using crude media instead of pure D-GalUA/glycerol mixtures seems to be relatively small.

3. Discussion

It has been a long-term challenge to successfully convert D-GalUA, an oxidized sugar derivative abundantly present in pectin-rich biomass residues to valuable products. The co-fermentation of the metabolizable carbon sources present in SBP or citrus peel waste hydrolysates to ethanol or other reduced chemicals has already been considered in the

past (Rezicó et al., 2013). However, an efficient valorization via this route has to take into account the fact that, from a degree of reduction perspective, none of the carbon sources endogenously present in pectinolytic waste allow for anaerobic, redox-neutral ethanol formation. In contrast, the reduced compound glycerol which is a by-product from different industries (Russmayer et al., 2019) represents an ideal co-substrate. Apart from this, the addition of glycerol to hydrolysates from pectin-rich biomass brings about an additional advantage. It will increase the carbon available in the feedstock that can be converted to ethanol. It is generally accepted that an economically viable ethanol production requires an ethanol concentration of at least 5% (v v^{-1}) for the distillation process, with higher titers being more beneficial. It can be easily calculated that the pectin-rich residues do not account for sufficiently high carbon availability. Here, we focused on equipping the popular yeast cell factory *S. cerevisiae* with the ability to ferment D-GalUA in the presence of glycerol.

Our current study unambiguously proves for the first time that ethanol formation from co-fermenting D-GalUA and glycerol is a realistic opportunity. In synthetic medium containing these two carbon sources

and by applying oxygen-limiting conditions, an ethanol yield of 0.48 ± 0.06 C-mol C-mol$_{substrate}^{-1}$ was realized which is 71% of the maximum theoretical yield. Another important achievement of the current study is the remarkably high specific D-GalUA consumption rate (up to 0.23 g g$_{CDW}^{-1}$ h^{-1}). Compared to the previous attempts aiming at D-GalUA utilization by engineered *S. cerevisiae,* the genetic modifications supporting glycerol catabolism (Ho et al., 2017, 2018) brought about by our baseline strain have certainly been a major prerequisite for the efficient D-GalUA utilization in the strain Gly/GalUA. As already mentioned, glycerol is one of the two central metabolites formed via the fungal D-GalUA pathway which need to be converted to ethanol. The modifications also allow efficient co-feeding of glycerol.

Due to its performance, the strain constructed in the current work has quite interesting characteristics for the development of aerobic processes and the production of biomass-related products such as proteins or lipids. It might also be used as a starting point to address fermentative processes. However, its inability to co-ferment D-GalUA and glycerol to high ethanol titers and yields is a major limitation of the current strain for ethanol production from pectin-rich residues using the traditional ethanol production conditions.

Although neutral with regard to electrons, it is obvious that our Gly/ GalUA strain is not yet balanced in terms of co-factors. In fact, there is a lack of efficient enzyme variants for D-galacturonate and L-glyceraldehyde reductases with a preference for NADH over NADPH. It should also be noted that we did not consider the current scenario completely unpromising. In fact, we do not exactly know whether i) the co-catabolism of glycerol and D-GalUA provides additional sources of cytosolic NADPH, ii) the D-galacturonate reductase (GaaA) consumes NADH or NADPH *in vivo* under the thermodynamic constraints in the current strain (the rate of cytosolic NADH generation is supposed to be relatively high in a DHA pathway strain), and iii) the multiple genetic modifications in the strain Gly/GalUA create the possibility of metabolic reactions that lead to the net conversion of NAD$^+$/NADH to NADP$^+$/ NADPH. Unlike bacteria, baker's yeast does not exhibit a transhydrogenase (Bakker et al., 2001). During growth on D-glucose, the oxidative pentose phosphate pathway (oxPPP) and the aldehyde dehydrogenase Ald6 are known to be the major routes of NADPH regeneration in *S. cerevisiae.* Conversely, cells have been shown to switch to isocitrate dehydrogenase (Idp2) and Ald6 during growth on acetate or ethanol since oxPPP is the energetically unfavorable on C2 carbon sources (Grabowska and Chelstowska, 2003; Meaden et al., 1997; Minard and McAlister-Henn, 2005). In contrast, there is virtually no information in the literature about the major sources of cytosolic NADPH during growth on glycerol as the sole carbon source. Regardless, because the D-GalUA consumption rate was fairly high, it seems that NADPH must have been efficiently regenerated in our strain. We hypothesized the oxPPP to be the most likely route of NADPH regeneration in our Gly/GalUA strain when co-utilizing glycerol and D-GalUA. Indeed, feeding ^{13}C glycerol allowed us to confirm this theory because it also led to significant labeling in the P5P (pentose 5-phosphate) m+4 pool, i.e. in the lumped pentose phosphate pool (see Supplementary Fig. 7). Together with the fact that a strain with a disrupted glucose 6-phosphate dehydrogenase (*zwf1Δ*) was not able to grow on glycerol and D-GalUA (data not shown), we qualify these findings as strong hints for active gluconeogenesis while growing on glycerol. It is plausible that the strong expression of the heterologous D-GalUA transporter caused a rapid uptake of the sugar acid so that cells had to deal with a high influx of both glycerol and D-GalUA concomitantly. The assumed high rate of NADH generation in the cytosol by the DHA pathway could be a strong driving force for rapidly reducing the D-GalUA into L-GalA, the first intermediate of the fungal GalUA pathway. Nonetheless, the second reductase in the pathway (GaaD) is strictly NADPH dependent (Fig. 1b). If the NADPH was mainly generated via the oxPPP, this would require gluconeogenesis and a net loss of carbon due to carbon dioxide formation. Moreover, the net ATP gain would be lower. A more detailed metabolic flux analysis is required to verify this assumption. In any case, it might be a promising

future endeavor to create a fungal D-GalUA pathway with two reductases that can utilize/prefer NADH as electron donor. Thus, the work of Harth et al. (2020) who used protein engineering to switch co-factor preference of the first reductase in the pathway can be considered as a promising step in the right direction.

Although an NADH-dependent D-GalUA catabolic pathway might overcome metabolic imbalances and the assumed forced detour via the oxPPP accompanied by net ATP loss, one still has to consider that both glycerol and D-GalUA are 'non-fermentable' as far as is known for all wild-type fungal organisms, i.e. central carbon metabolism is fully respiratory. Efficient ethanol production requires high glycolytic rates that result in ethanol formation. This naturally occurs in the Crabtree-positive yeast *S. cerevisiae* (even under aerobic conditions) when it grows on excess D-glucose (Crabtree, 1929; Thiere and Penninckx, 2010). However, significantly decreased activities of pyruvate decarboxylase and alcohol dehydrogenase have been reported when *S. cerevisiae* grows on non-fermentable carbon sources (Boles and Zimmermann, 1993; Denis et al., 1983). The fact that these two enzymes are not upregulated during co-catabolism of D-GalUA/glycerol might explain pyruvate accumulation in the Gly/GalUA strain (Fig. 6b).

We want to mention that we expected significantly higher ethanol titers and yields based on the values obtained from glycerol alone in the study of Aβkamp et al. (2019). However, a different strain background (CBS 6412-13A) was used in the respective study for the construction of the 'DHA pathway strains', and we have good reasons to believe that the genetic background strongly influenced the manifestation of ethanol formation in DHA pathway strains (unpublished data). This fact has been unknown at the beginning of the current study when we decided to use the CEN.PK derivative due to its high specific growth rate in synthetic glycerol medium (Ho et al., 2018; Klein et al., 2016a). The establishment of the GalUA pathway in the latter baseline strain is pending due to a much lower transformation efficiency.

In conclusion, the D-GalUA/(crude) glycerol co-utlization and co-fermentation concept presented here and the knowledge gained from our constructed *S. cerevisiae* strain Gly/GalUA holds great potential for developing future industrial processes using hydrolysates of pectin–rich agricultural residues as feedstock. The strain seems to be robust in crude substrate and a pH of 4.5. Apart from equipping the strain with a functional catabolic pathway for arabinose utilization, metabolic engineering that support the switch from respiration to fermentation combined with the establishment of an NADH-dependent GalUA catabolic pathway are suggested to be promising next steps towards the envisaged long-term goal of co-fermenting the carbon sources to valuable fermentation products. Apart from its robustness to inhibitors present in crude substrates, the fact that *S. cerevisiae* is naturally prone to fermentative metabolism and can grow under anaerobic conditions makes it a promising future endeavor.

4. Methods

4.1. Strains, plasmids and strain maintenance

All strains and plasmids used in this study are listed in Supplementary Tables 2 and 3, respectively. *S. cerevisiae* strains were routinely maintained in YPD medium containing 10 g L^{-1} yeast extract, 20 g L^{-1} peptone, 20 g L^{-1} dextrose (15 g L^{-1} agar was added for solid medium). If required, the medium was supplemented with nourseothricin (100 mg mL^{-1}) or hygromycin B (300 mg mL^{-1}) for selection purposes. *E. coli* DH5α was used for plasmid propagation; cells were routinely grown in lysogeny broth (LB) containing 10 g L^{-1} peptone, 5 g L^{-1} yeast extract and 10 g L^{-1} NaCl (pH 7.0) supplemented with 15 g L^{-1} agar for solid medium. For selection and maintenance of plasmid-containing cells, the medium was supplemented with 100 mg mL^{-1} ampicillin. Cultivations of *S. cerevisiae* and *E. coli* were performed at 30 ℃ and 37 ℃, respectively. Cultivations in liquid media were carried out using an orbital shaker at 200 rpm unless otherwise specified. Plasmids were isolated from *E. coli*

using the GeneJET Plasmid Miniprep Kit (Thermo Fisher Scientific, Massachusetts, USA).

4.2. General molecular biology techniques

PCR primers used in the current study can be found in Supplementary Tables 4 and 5 Preparative PCRs for cloning were performed using Phusion® High-Fidelity DNA Polymerase (New England Biolabs, Frankfurt am Main, Germany) or Kappa HiFi DNA Polymerase (Roche Sequencing Solutions, California, USA) according to the manufacturer's instructions. PCR products were purified using the GeneJET PCR purification Kit (Thermo Fisher Scientific, Massachusetts, USA).

4.3. Genetic modifications of Saccharomyces cerevisiae

In order to integrate the expression cassettes for the fungal GalUA pathway into the Gly reference strain (Supplementary Table 2) via CRISPR/Cas9, the strain was first transformed with the plasmid p414-TEF1p-Cas9-CYC1t-nat1. Eight of the nine repair fragments (I to IV and VI to VIIII) shown in Fig. 1c were PCR-amplified from plasmids shown in Supplementary Table 3 using the respective primers. Solely fragment V was PCR-amplified (primer pair 1328/1329) from genomic DNA isolated from strain CEN.PK113-7D *UBR2$_{JL1}$ GUT1$_{JL1}$* (Supplementary Table S1). All primers were provided with 5′ overhangs generating 40–60 bp homologous arms to sequences up and downstream of *YPRCτ3* genomic region or to the respective adjacent fragment(s). The nine fragments were transferred together with the plasmid p426-SNR52p-gRNA.YPRCτ3-SUP4t-hphMX (Xiberras et al., 2020) into the *S. cerevisiae* strain Gly reference equipped with the plasmid-based Cas9 expression. Transformation of *S. cerevisiae* with plasmids or linear integration cassettes was performed according to the lithium acetate – carrier DNA method (Gietz et al., 1995). Correct integration of all fragments was verified by isolating genomic DNA from transformants and applying diagnostic PCR using OneTaq® QuickLoad® DNA Polymerase and buffer according to the manufacturer's guidelines (New England Biolabs, Frankfurt am Main, Germany). PCR primers were designed to bind upstream and downstream of the genomic integration site as well as within the integrated fragments/expression cassettes. Due to the presence of multiple cassettes, additional primers were designed to produce amplicons covering the junctions between the individual integrated fragments.

4.4. Isolation of genomic DNA from S. cerevisiae

Single colonies on YPD agar plates were used to isolate genomic DNA used as template for PCR. Approximately 50 mg of cells were suspended in 200 μL of TE buffer (10 mM Tris, 1 mM EDTA, pH 8.0). Subsequently, 300 mg of acid-washed glass beads with a diameter of 0.425–0.6 mm and 200 μL of a mix containing phenol, chloroform and isoamyl alcohol in a ratio of 25:24:1 were added. The tubes were vortexed at maximum speed for 2 min and centrifuged at 15700 *g* for 10 min according to a protocol modified from Hoffman and Winston (1987). For 25 μl PCR reactions, 1 μL of a 1:10 dilution (in dH$_2$O) of the resulting aqueous phase was used as template.

4.5. Media used for physiological characterization of engineered S. cerevisiae

Three different types of media were used in the current study: i) defined synthetic medium according to Verduyn et al. (1992), ii) complex medium based on real SBP hydrolysate and iii) defined synthetic medium based on YNB and mimicking the carbon source composition of SBP hydrolysates. The defined synthetic Verduyn medium was used with D-glucose (SM$_{Glu}$), D-GalUA (SM$_{D-GalUA}$) or with glycerol (SM$_{Gly}$) as the sole carbon source. SM$_{Glu}$ contained 5 g L^{-1} (NH$_4$)$_2$SO$_4$, 3 g L^{-1} KH$_2$PO$_4$, 0.5 g L^{-1} MgSO$_4$·7H$_2$O, 15 mg L^{-1} EDTA, 4.5 mg L^{-1} ZnSO$_4$·7H$_2$O, 0.84

mg L^{-1} MnCl$_2$·2H$_2$O, 0.3 mg L^{-1} CoCl$_2$·6H$_2$O, 0.3 mg L^{-1} CuSO$_4$·5H$_2$O, 0.4 mg L^{-1} NaMoO$_4$·2H$_2$O, 4.5 mg L^{-1} CaCl$_2$·2H$_2$O, 3 mg L^{-1} FeSO$_4$·7H$_2$O, 1 mg L^{-1} H$_3$BO$_3$, and 0.1 mg L^{-1} KI. After heat sterilization the following vitamins were added: 0.05 mg L^{-1} D-(+)-biotin, 1 mg L^{-1} D-pantothenic acid hemicalcium salt, 1 mg L^{-1} nicotinic acid, 25 mg L^{-1} myo-inositol, 1 mg L^{-1} thiamine chloride hydrochloride, 1 mg L^{-1} pyridoxine hydro-chloride, and 0.2 mg L^{-1} 4-aminobenzoic acid. For preparing SM$_{Glu}$ medium, 20 g L^{-1} D-glucose was added and the pH was adjusted to 6.5 with 4 M KOH. For preparing SM$_{Gly}$, the (NH$_4$)$_2$SO$_4$ was replaced with 2.27 g L^{-1} of urea (CH$_4$N$_2$O), which contains an equivalent amount of nitrogen. Moreover, D-glucose was replaced by 75 g L^{-1} (equivalent to 6% v v^{-1}) pure glycerol. The pH of the latter medium was set to 5.0 using 4 M KOH. D-GalUA was added to SM$_{Gly}$ medium at the indicated concentration. For the spiking experiment, 2.5 mL D-GalUA was added from a filter-sterilized stock solution of 440 g L^{-1} D-GalUA to the cultures grown in 100 mL SM$_{Gly}$.

Defined media based on 6.7 g L^{-1} Yeast Nitrogen Base (YNB) contained amino acids (10 mg L^{-1} of L-histidine, 20 mg L^{-1} of DL-methionine and 20 mg L^{-1} of DL-tryptophan) and ammonium sulfate. The defined synthetic hydrolysate that mimicked the carbon source composition of SBP hydrolysate was prepared with YNB$_{waa}$ and contained D-GalUA (9 g L^{-1}), D-glucose (5 g L^{-1}), D-galactose (2 g L^{-1}), L-arabinose (9 g L^{-1}) and acetic acid (30 mM). Unless otherwise specified, the pre-cultivation medium for the experiments in synthetic hydrolysates contained YNB$_{w/oaa}$ supplemented with D-glucose (e.g. YNB$_{w/oaaGlu}$).

For the experiments using crude SBP hydrolysate obtained by enzymatic treatment (see below) and pure glycerol, the SBP hydrolysate was supplemented with 6.7 g L^{-1} of Yeast Nitrogen Base (YNB) with amino acids (i.e. 10 mg L^{-1} of L-histidine, 20 mg L^{-1} of DL-methionine and 20 mg L^{-1} of DL-tryptophan). In the experiments using SBP hydrolysate and crude glycerol, the SBP hydrolysate was supplemented with 2.7 g L^{-1} urea and crude glycerol. The crude glycerol containing 82% (w v^{-1}) glycerol was kindly provided by a biodiesel company and added to the medium to obtain a glycerol concentration of 50 g L^{-1}. The pH was adjusted to the indicated value using 5 M NaOH or 4 M KOH respectively.

4.6. Preparation of hydrolysate from SBP

Pressed sugar beet pulp from the 2017 sugar beet campaign was a kind gift from Tiense Suikerraffinadarij N.V. Raffinerie Tirlemontoise S. A. (Belgium). For preparation of SBP hydrolysate, a 10 L fermenter reaction vessel was filled with 2.67 kg (wet weight) of SBP and water was added to a volume of 9 L. This corresponds to approximately 5.5% (w v^{-1}) total solid density. The vessel with the SBP was autoclaved (20 min, 121 °C) and connected to the controller of a Biostat B fermenter (Sartorius, Göttingen, Germany). Enzymatic hydrolysis was started by addition of 5 mL Viscozyme L and 5 mL Celluclast (Sigma-Aldrich, Missouri, USA) and continuous stirring at 4000 rpm at 40 °C. Prior to use, the commercial enzyme preparations were deprived of low molecular mass solutes by gel filtration chromatography with a PD-10 desalting column (GE Healthcare, Chicago, USA) using 25 mM sodium phosphate buffer pH 6.0 as the eluent, resulting in a 1.4-fold dilution of the original enzyme cocktails, and were filtered with a FiltropurS PES 0.45 μm syringe filter (Sarstedt, Nümbrecht, Germany). After 24 h, another 5 mL each of the Viscozyme L and Celluclast preparations was added followed by further incubation (40 °C, 4000 rpm) after which most of the particulate material was degraded. After centrifugation (20 min, 5400 *g*) the supernatant was filtered using Whatman Folded Filters 597½ (GE Healthcare, Chicago, USA) followed by filter-sterilization with a 0.2 μm Flow Bottle Top Filter (Thermo Fisher Scientific, Massachusetts, USA).

The various sugar components present in the SBP hydrolysate were determined after appropriate dilution with water by high performance anion exchange chromatography with pulsed amperometric detection (HPAEC-PAD) using a Dionex ICS-3000 ion chromatography system

equipped with a CarboPac™ PA1 column (Thermo Fisher Scientific) as described (Mechelke et al., 2017). Chromatography was performed at a constant temperature of 30 °C, using a linear 7.5–100 mM sodium acetate gradient in 100 mM sodium hydroxide at a flow rate of 1 mL min^{-1}. Quantification of monosaccharides was done by calibration curves generated via separation of defined amounts of analytical grade standards purchased from Sigma-Aldrich except for L-(+)-arabinose (Carl Roth GmbH & Co KG, Karlsruhe, Germany) and D-(+)-GalUA (Merck Millipore GmbH, Düsseldorf, Germany). The concentrations of acetate, methanol and ethanol were measured via gas chromatography with a GC-2010 apparatus (Shimadzu) with flame ionization detection (GC-FID). The samples (1 µL) were separated using a temperature gradient from 50 to 250 °C with a Stabilwax capillary column (60 m length, 0.32 mm inner diameter, 0.5 µm film thickness; Restek, Pennsylvania, USA) and nitrogen as carrier gas. 1-propanol (0.05%) was used as an internal standard. The composition of the hydrolysate SBP4H13 which was used in this study is shown in Fig. 1a. The pH of the hydrolysate (before adjustment) was 2.3.

4.7. Batch shake flask cultivations

Unless otherwise stated, the filling volume of the Erlenmeyer flasks was 20% and the cultures were incubated at 30 °C at the indicated shaking speed. Pre-cultivated cells were harvested by centrifugation at 800*g* for 5 min and (if indicated) washed once in the main culture medium or in distilled water and inoculated at the indicated initial cell density.

4.8. Quantification of extracellular metabolites

Batch cultivation derived samples were centrifuged in a microcentrifuge MiniSpin Plus (Eppendorf) (6700 *g* 3 min) and 100 µL of the supernatant was pipetted into high-performance liquid chromatography (HPLC) vials and diluted with 900 µL 50 mM H$_2$SO$_4$ solution. The concentration of D-GalUA, D-glucose, D-galactose, L-arabinose, glycerol, acetic acid and ethanol in each sample was determined by HPLC (Hitachi LabChrom Elite), using a column Aminex HPX-87H (Bio-Rad München, Germany) coupled with UV/visible detector (for organic acids) and refractive index detector (for sugars and ethanol). The retention times for D-GalUA, D-glucose, D-galactose, L-arabinose, glycerol, acetic acid and ethanol were 8.2, 9, 9.6, 10.3, 13.4, 14.4 and 21.3 min respectively. Elution of the compounds was performed with 5 mM H$_2$SO$_4$ at a flow rate of 0.6 mL min^{-1} for 30 min. Column temperature was set to 65 °C. Concentrations of metabolites were calculated using calibration curves for each compound.

4.9. ^{13}C labelling experiment and sample processing for intracellular metabolome analysis

S. cerevisiae Gly/GalUA was grown in SM$_{Gly}$ medium. Pre-cultures were expanded in shake flask at 30 °C, 200 rpm and a starting pH of 5.0 with initial biomass density of 0.9–1 g$_{CDW}$ L^{-1} from 5 mL working volume to 100 mL working volume. Before performing the isotopic tracer study, cells were cultivated with initial glycerol concentration (non-labelled) of 75 g L^{-1}. Cells were harvested by centrifugation (5 min, 4 °C, and 8000 *g*) and subsequently washed with isotonic 0.9% (w v^{-1}) sodium chloride solution to remove residual non-labelled glycerol. Next, defined cell amounts were resuspended in a modified minimal media with 30 g L^{-1} [U–^{13}C$_3$]-glycerol (Euroisotope, Saarbrücken, Germany) only (reference culture) or 30 g L^{-1} [U–^{13}C$_3$]-glycerol and 12 g L^{-1} [U–^{12}C$_6$]-D-GalUA as carbon source(s). After the transfer, the cultures yielded an initial biomass concentration of 5.5–6.5 g$_{DW}$ L^{-1}. The cultivation conditions for carbon labelling experiments are exactly the same as the precultures: 30 °C temperature, 200 rpm shaking speed, and 20% of cultures working volume.

Samples for intracellular pyruvate quantification (2 mL cell suspension, 10–15 mg of total CDW) were drawn aseptically from three biological replicates (n = 3) and quenched immediately by injection in 5 mL precooled methanol (−70 °C) according to Canelas et al. (2009). Sampling intervals were successively prolonged from 15 min within the first hour to 1 h, 2 h, and 24 h to capture the fast ^{13}C labelling dynamics. Cell pellets were collected by centrifugation (1000 *g* at −11 °C for 10 min) and quenching supernatants were carefully discarded. Remaining pellets were washed again with 5 mL precooled methanol (−70 °C). After addition of L-Norvaline as internal standard, the cell pellets were temporarily stored at −70 °C. The enzymatic inactivation of samples and preparation of intracellular extracts were performed using a cold extraction approach according to the methodology by Patil et al. (2021). Prior to extraction, a certain amount of 50% (v v^{-1}) MeOH/H$_2$O precooled at −20 °C was added to each sample to achieve a constant biomass concentration (50 g$_{CDW}$ L^{-1}) in the final extraction suspension. Cell pellets were resuspended by rotational vortexing (~1 min) and chilling in a cooled cryostat (−40 °C) to achieve homogenous suspensions with a temperature below −20 °C. Next, an equivoluminal amount of chloroform (precooled at −20 °C) was added and the extraction was performed with rotary overhead-shaker for 1 h at −20 °C and 1 h at room temperature. The remaining cell debris and chloroform were separated via centrifugation (1000 *g* at 4 °C for 10 min). and the upper aqueous methanol phase (polar metabolites) was isolated and stored at −70 °C for further analysis.

4.10. LC-MS based quantification and ^{13}C labelling analysis of intracellular pyruvate pools

Targeted metabolome analyses of intracellular extracts were based on former HILIC-ESI-MS/MS studies (Feith et al., 2019; Teleki et al., 2015) using an Agilent 6410B Triple-Quad LC-MS/MS platform with an electrospray ion (ESI) source. System control, acquisition and analysis of data were performed by usage of commercial MassHunter B.06.00 software. Measurement of pyruvate isotopologues was performed using a protocol established by Junghans et al. (2019). Cell extracts containing pyruvate were derivatized with phenylhydrazine as described by Zimmermann et al. (2014). Mass isotopomers were analyzed using an Agilent 1200 HPLC system based on a bicratic ion-pair RPLC method (Hypersil™ BDS C18 column 15 cm × 4.6 mm, 3 µm equipped with a Hypersil™ BDS guard column 10 × 4 mm, 5 µm). Analysis was conducted with selected ion monitoring (SIM) mode using pre-optimized precursor ion transition (0.3 u) with adapted MS parameters and ESI conditions (Feith et al., 2019). Absolute quantification of pyruvate pools was performed using a spiking method for selected samples with external standards.

CRediT author statement

Andreea Perpelea: Conceptualization, Investigation, Methodology, Formal analysis, Writing – Original Draft and Review & Editing, Visualization. **Andy Wiranata Wijaya:** Investigation, Formal analysis **Luís C. Martins:** Investigation. **Dorthe Rippert:** Investigation. **Mathias Klein:** Formal analysis, Writing – Original Draft. **Angel Angelov:** Investigation, Methodology. **Kaisa Peltonen:** Resources **Attila Teleki:** Investigation. **Wolfgang Liebl:** Resources, Funding acquisition, Supervision **Peter Richard:** Resources, Funding acquisition, Supervision. **Johan M. Thevelein:** Funding acquisition, Writing – Original Draft. **Ralf Takors:** Supervision. **Isabel Sá Correia:** Writing – Original Draft, Funding acquisition, Supervision. **Elke Nevoigt:** Conceptualization, Writing – Original Draft and Review & Editing, Visualization, Project administration, Funding acquisition, Supervision.

Declaration of competing interest

The authors declare that there are no competing interests.

Acknowledgements

Appendix A. Supplementary data

Supplementary data to this article can be found online at https://doi.org/10.1016/j.ymben.2021.10.001.

References

Alazi, E., Khosravi, C., Homan, T.G., du Pré, S., Arentshorst, M., di Falco, M., Pham, T.T. M., Peng, M., Aguilar-Pontes, M.V., Visser, J., Tsang, A., de Vries, R.P., Ram, A.F.J., 2017. The pathway intermediate 2-keto-3-deoxy-L-galactonate mediates the induction of genes involved in D-galacturonic acid utilization in *Aspergillus niger*. FEBS Lett. 591, 1408–1418. https://doi.org/10.1002/1873-3468.12654.

Aßkamp, M.R., Klein, M., Nevoigt, E., 2019. *Saccharomyces cerevisiae* exhibiting a modified route for uptake and catabolism of glycerol forms significant amounts of ethanol from this carbon source considered as "non-fermentable. Biotechnol. Biofuels 12, 257. https://doi.org/10.1186/s13068-019-1597-2.

Bakker, B.M., Overkamp, K.M., van Maris, A.J.A., Kötter, P., Luttik, M.A.H., van Dijken, J.P., Pronk, J.T., 2001. Stoichiometry and compartmentation of NADH metabolism in *Saccharomyces cerevisiae*. FEMS (Fed. Eur. Microbiol. Soc.) Microbiol. Rev. 25, 15–37. https://doi.org/10.1111/j.1574-6976.2001.tb00570.x.

Benz, J.P., Protzko, R.J., Andrich, J.M.S., Bauer, S., Dueber, J.E., Somerville, C.R., 2014. Identification and characterization of a galacturonic acid transporter from *Neurospora crassa* and its application for *Saccharomyces cerevisiae* fermentation processes. Biotechnol. Biofuels 7, 1–13. https://doi.org/10.1186/1754-6834-7-20.

Berlowska, J., Binczarski, M., Dziugan, P., Wilkowska, A., Kregiel, D., Witonska, I., 2018. Sugar beet pulp as a source of valuable biotechnological products. Advances in Biotechnology for Food Industry 14, 359–392. https://doi.org/10.1016/B978-0-12-811443-8.00013-X.

Berlowska, J., Pielech-Przybylska, K., Balcerek, M., Cieciura, W., Borowski, S., Kregiel, D., 2017. Integrated bioethanol fermentation/anaerobic digestion for valorization of sugar beet pulp 10. Energies 1255. https://doi.org/10.3390/en10091255.

Biz, A., Sugai-Guérios, M.H., Kuivanen, J., Maaheimo, H., Krieger, N., Mitchell, D.A., Richard, P., 2016. The introduction of the fungal d-galacturonate pathway enables the consumption of d-galacturonic acid by *Saccharomyces cerevisiae* 15. Microbial Cell Factories, p. 144. https://doi.org/10.1186/s12934-016-0544-1.

Boles, E., Zimmermann, F.K., 1993. Induction of pyruvate decarboxylase in glycolysis mutants of *Saccharomyces cerevisiae* correlates with the concentrations of three-carbon glycolytic metabolites. Arch. Microbiol. 160, 324–328. https://doi.org/10.1007/BF00292085.

Borodina, I., Nielsen, J., 2014. Advances in metabolic engineering of yeast *Saccharomyces cerevisiae* for production of chemicals 9, 609–620. Biotechnol. J. https://doi.org/10.1002/biot.201300445.

Burk, M.J., van Dien, S., 2016. Biotechnology for chemical production: challenges and opportunities. Trends Biotechnol. 34, 187–190. https://doi.org/10.1016/j.tibtech.2015.10.007.

Canelas, A.B., ten Pierick, A., Ras, C., Seifar, R.M., van Dam, J.C., van Gulik, W.M., Heijnen, J.J., 2009. Quantitative evaluation of intracellular metabolite extraction techniques for yeast metabolomics. Anal. Chem. 81, 7379–7389. https://doi.org/10.1021/ac900999t.

Chroumpi, T., Mäkelä, M.R., de Vries, R.P., 2020. Engineering of Primary Carbon Metabolism in Filamentous Fungi, vol. 43, p. 107551. https://doi.org/10.1016/j.biotechadv.2020.107551.

Crabtree, H.G., 1929. Observations on the carbohydrate metabolism of tumours. Biochem. J. 23, 536–545. https://doi.org/10.1042/bj0230536.

Cunha, J.T., Soares, P.O., Romaní, A., Thevelein, J.M., Domingues, L., 2019. Xylose fermentation efficiency of industrial *Saccharomyces cerevisiae* yeast with separate or combined xylose reductase/xylitol dehydrogenase and xylose isomerase pathways. Biotechnol. Biofuels 12, 1–14. https://doi.org/10.1186/s13068-019-1360-8.

da Silva, G.P., Mack, M., Contiero, J., 2009. Glycerol: a promising and abundant carbon source for industrial microbiology. Biotechnol. Adv. 27, 30–39. https://doi.org/10.1016/j.biotechadv.2008.07.006.

Denis, C.L., Ferguson, J., Young, E.T., 1983. mRNA levels for the fermentative alcohol dehydrogenase of *Saccharomyces cerevisiae* decrease. J. Biol. Chem. 258, 1165–1171. https://doi.org/10.1016/S0021-9258(18)33174-0.

Duwe, A., Tippkötter, N., Ulber, R., 2019. Lignocellulose-biorefinery: ethanol-focused. In: Wagemann, K., Tippkötter, N. (Eds.), Biorefineries. Advances in Biochemical Engineering/Biotechnology, vol. 166. Springer, Cham. https://doi.org/10.1007/10_2016_72.

Edwards, M.C., Doran-Peterson, J., 2012. Pectin-rich biomass as feedstock for fuel ethanol production. Appl. Microbiol. Biotechnol. 95, 565–575. https://doi.org/10.1007/s00253-012-4173-2.

Expanding biocatalysis for a sustainable future. Nature Catalysis 3, 2020, 179–180. https://doi.org/10.1038/s41929-020-0447-8.

Faostat. n.d. http://www.fao.org/faostat/en/#data/QC. accessed 4.12.20.

Feith, A., Teleki, A., Graf, M., Favilli, L., Takors, R., 2019. HILIC-enabled ^{13}C metabolomics strategies: comparing quantitative precision and spectral accuracy of QTOF high- and QQQ low-resolution mass spectrometry. Metabolites 9, 63. https://doi.org/10.3390/metabo9040063.

Flagfeldt, D.B., Siewers, V., Huang, L., Nielsen, J., 2009. Characterization of chromosomal integration sites for heterologous gene expression in *Saccharomyces cerevisiae*. Yeast 26, 545–551. https://doi.org/10.1002/yea.1705.

Francois, J.M., Alkim, C., Morin, N., 2020. Engineering microbial pathways for production of bio-based chemicals from lignocellulosic sugars: current status and perspectives. Biotechnol. Biofuels 13, 118. https://doi.org/10.1186/s13068-020-01744-6.

Gama, R., van Dyk, J.S., Pletschke, B.I., 2015. Optimisation of enzymatic hydrolysis of apple pomace for production of biofuel and biorefinery chemicals using commercial enzymes. 3 Biotech 5, 1075–1087. https://doi.org/10.1007/s13205-015-0312-7.

Geisendorf, S., Pietrulla, F., 2018. The circular economy and circular economic concepts-a literature analysis and redefinition. Thunderbird Int. Bus. Rev. 60, 771–782. https://doi.org/10.1002/tie.21924.

Gietz, R.D., Schiestl, R.H., Willems, A.R., Woods, R.A., 1995. Studies on the transformation of intact yeast cells by the LiAc/SS-DNA/PEG procedure. Yeast 11, 355–360. https://doi.org/10.1002/yea.320110408.

Grabowska, D., Chelstowska, A., 2003. The *ALD6* gene product is indispensable for providing NADPH in yeast cells lacking glucose-6-phosphate dehydrogenase activity. J. Biol. Chem. 278, 13984–13988. https://doi.org/10.1074/jbc.M210076200.

Grohmann, K., Manthey, J.A., Cameron, R.G., Buslig, B.S., 1999. Purification of citrus peel juice and molasses. J. Agric. Food Chem. 47, 4859–4867. https://doi.org/10.1021/jf9903049.

Günan Yücel, H., Aksu, Z., 2015. Ethanol fermentation characteristics of *Pichia stipitis* yeast from sugar beet pulp hydrolysate: use of new detoxification methods. Fuel 158, 793–799. https://doi.org/10.1016/j.fuel.2015.06.016.

Hagman, A., Piškur, J., 2015. A study on the fundamental mechanism and the evolutionary driving forces behind aerobic fermentation in yeast. PLoS One 10, e0116942. https://doi.org/10.1371/journal.pone.0116942.

Hamley-Bennett, C., Lye, G.J., Leak, D.J., 2016. Selective fractionation of Sugar Beet Pulp for release of fermentation and chemical feedstocks; optimisation of thermo-chemical pre-treatment. Bioresour. Technol. 209, 259–264. https://doi.org/10.1016/j.biortech.2016.02.131.

Harth, S., Wagner, J., Sens, T., Choe, J. yong, Benz, J.P., Weuster-Botz, D., Oreb, M., 2020. Engineering cofactor supply and NADH-dependent d-galacturonic acid reductases for redox-balanced production of l-galactonate in *Saccharomyces cerevisiae*. Sci. Rep. 10, 19021. https://doi.org/10.1038/s41598-020-75926-5.

Hilditch, S., Berghäll, S., Kalkkinen, N., Penttilä, M., Richard, P., 2007. The missing link in the fungal D-galacturonate pathway: identification of the L-threo-3-deoxy-hexulosonate aldolase. J. Biol. Chem. 282, 26195–26201. https://doi.org/10.1074/jbc.M704401200.

Ho, P.W., Klein, M., Futschik, M., Nevoigt, E., 2018. Glycerol positive promoters for tailored metabolic engineering of the yeast *Saccharomyces cerevisiae*. FEMS Yeast Res. 18, foy019. https://doi.org/10.1093/femsyr/foy019.

Ho, P.-W., Swinnen, S., Duitama, J., Nevoigt, E., 2017. The sole introduction of two single-point mutations establishes glycerol utilization in *Saccharomyces cerevisiae* CEN.PK derivatives. Biotechnol. Biofuels 10, 10. https://doi.org/10.1186/s13068-016-0696-6.

Hoffman, C.S., Winston, F., 1987. A ten-minute DNA preparation from yeast efficiently releases autonomous plasmids for transformation of *Escherichia coli*. Gene 57, 267–272. https://doi.org/10.1016/0378-1119(87)90131-4.

Hong, K.K., Nielsen, J., 2012. Metabolic engineering of *Saccharomyces cerevisiae*: a key cell factory platform for future biorefineries. Cell. Mol. Life Sci. 69, 2671–2690. https://doi.org/10.1007/s00018-012-0945-1.

Huisjes, E.H., de Hulster, E., van Dam, J.C., Pronk, J.T., van Maris, A.J.A., 2012a. Galacturonic acid inhibits the growth of *Saccharomyces cerevisiae* on galactose, xylose, and arabinose. Appl. Environ. Microbiol. 78, 5052–5059. https://doi.org/10.1128/AEM.07617-11.

Huisjes, E.H., Luttik, M.A.H., Almering, M.J.H., Bisschops, M.M.M., Dang, D.H.N., Kleerebezem, M., Siezen, R., van Maris, A.J.A., Pronk, J.T., 2012b. Toward pectin fermentation by *Saccharomyces cerevisiae*: expression of the first two steps of a bacterial pathway for D-galacturonate metabolism. J. Biotechnol. 162, 303–310. https://doi.org/10.1016/j.jbiotec.2012.10.003.

Islam, Z. ul, Klein, M., Aßkamp, M.R., Ødum, A.S.R., Nevoigt, E., 2017. A modular metabolic engineering approach for the production of 1,2-propanediol from glycerol by *Saccharomyces cerevisiae*. Metab. Eng. 44, 223–235. https://doi.org/10.1016/j.ymben.2017.10.002.

Jeong, D., Park, H., Jang, B.-K., Ju, Y., Shin, M.H., Oh, E.J., Lee, E.J., Kim, S.R., 2021. Recent advances in the biological valorization of citrus peel waste into fuels and

chemicals. Bioresour. Technol. 323, 124603. https://doi.org/10.1016/j.biortech.2020.124603.

Jeong, D., Ye, S., Park, H., Kim, S.R., 2020. Simultaneous fermentation of galacturonic acid and five-carbon sugars by engineered *Saccharomyces cerevisiae*. Bioresour. Technol. 295, 122259. https://doi.org/10.1016/j.biortech.2019.122259.

John, I., Muthukumar, K., Arunagiri, A., 2017. A review on the potential of citrus waste for D-Limonene, pectin, and bioethanol production. Int. J. Green Energy 14, 599–612. https://doi.org/10.1080/15435075.2017.1307753.

Junghans, L., Teleki, A., Wijaya, A.W., Becker, M., Schweikert, M., Takors, R., 2019. From nutritional wealth to autophagy: in vivo metabolic dynamics in the cytosol, mitochondrion and shuttles of IgG producing CHO cells. Metab. Eng. 54, 145–159. https://doi.org/10.1016/j.ymben.2019.02.005.

Klein, M., Carrillo, M., Xiberras, J., Islam, Z. ul, Swinnen, S., Nevoigt, E., 2016a. Towards the exploitation of glycerol's high reducing power in *Saccharomyces cerevisiae*-based bioprocesses. Metab. Eng. 38, 464–472. https://doi.org/10.1016/j.ymben.2016.10.008.

Klein, M., Islam, Z. ul, Knudsen, P.B., Carrillo, M., Swinnen, S., Workman, M., Nevoigt, E., 2016b. The expression of glycerol facilitators from various yeast species improves growth on glycerol of *Saccharomyces cerevisiae*. Metabolic Engineering Communications 3, 252–257. https://doi.org/10.1016/j.meteno.2016.09.001.

Klein, M., Swinnen, S., Thevelein, J.M., Nevoigt, E., 2017. Glycerol metabolism and transport in yeast and fungi: established knowledge and ambiguities. Environ. Microbiol. 19, 878–893. https://doi.org/10.1111/1462-2920.13617.

Kumar, L.R., Yellapu, S.K., Tyagi, R.D., Zhang, X., 2019. A review on variation in crude glycerol composition, bio-valorization of crude and purified glycerol as carbon source for lipid production. Bioresour. Technol. 293, 122155. https://doi.org/10.1016/j.biortech.2019.122155.

Kwak, S., Jin, Y.S., 2017. Production of fuels and chemicals from xylose by engineered *Saccharomyces cerevisiae*: a review and perspective. Microb. Cell Factories 16, 82. https://doi.org/10.1186/s12934-017-0694-9.

Legrand, 2015. Collection les guides techniques de l'IRBAB | Feedipedia, n.d. URL. https://www.feedipedia.org/node/24413. accessed 12.7.20.

Li, C., Gao, S., Wang, H., Li, X., Ong, K.L., Yang, X., Lin, C.S.K., 2018. Succinic acid production using a glycerol-based medium by an engineered strain of *Yarrowia lipolytica*: statistical optimization and preliminary economic feasibility study. Biochem. Eng. J. 137, 305–313. https://doi.org/10.1016/j.bej.2018.06.012.

Martens-Uzunova, E.S., Schaap, P.J., 2008. An evolutionary conserved d-galacturonic acid metabolic pathway operates across filamentous fungi capable of pectin degradation. Fungal Genet. Biol. 45, 1449–1457. https://doi.org/10.1016/j.fgb.2008.08.002.

Martins, L.C., Monteiro, C.C., Semedo, P.M., Sá-Correia, I., 2020. Valorisation of pectin-rich agro-industrial residues by yeasts: potential and challenges. Appl. Microbiol. Biotechnol. 104, 6527–6547. https://doi.org/10.1007/s00253-020-10697-7.

Meaden, P.G., Dickinson, F.M., Mifsud, A., Tessier, W., Westwater, J., Bussey, H., Midgley, M., 1997. The *ALD6* gene of *Saccharomyces cerevisiae* encodes a cytosolic, Mg^{2+}-activated acetaldehyde dehydrogenase. Yeast 13, 1319–1327. https://doi.org/10.1002/(SICI)1097-0061(199711)13:14<1319::AID-YEA183>3.0.CO;2-T.

Mechelke, M., Herlet, J., Benz, J.P., Schwarz, W.H., Zverlov, V.V., Liebl, W., Kornberger, P., 2017. HPAEC-PAD for oligosaccharide analysis—novel insights into analyte sensitivity and response stability. Anal. Bioanal. Chem. 409, 7169–7181. https://doi.org/10.1007/s00216-017-0678-y.

Merli, R., Preziosi, M., Acampora, A., 2018. How do scholars approach the circular economy? A systematic literature review. J. Clean. Prod. 178, 703–722. https://doi.org/10.1016/j.jclepro.2017.12.112.

Minard, K.I., McAlister-Henn, L., 2005. Sources of NADPH in yeast vary with carbon source. J. Biol. Chem. 280, 39890–39896. https://doi.org/10.1074/jbc.M509461200.

Müller-Maatsch, J., Bencivenni, M., Caligiani, A., Tedeschi, T., Bruggeman, G., Bosch, M., Petrusan, J., van Droogenbroeck, B., Elst, K., Sforza, S., 2016. Pectin content and composition from different food waste streams. Food Chem. 201, 37–45. https://doi.org/10.1016/j.foodchem.2016.01.012.

Nevoigt, E., 2008. Progress in metabolic engineering of *Saccharomyces cerevisiae*. Microbiol. Mol. Biol. Rev. 72, 379–412. https://doi.org/10.1128/MMBR.00025-07.

Nielsen, J., Keasling, J.D., 2016. Engineering cellular metabolism. Cell 164, 1185–1197. https://doi.org/10.1016/j.cell.2016.02.004.

Palma, M., Guerreiro, J.F., Sá-Correia, I., 2018. Adaptive response and tolerance to acetic acid in *Saccharomyces cerevisiae* and *Zygosaccharomyces bailii*: a physiological genomics perspective. Front. Microbiol. 9, 274. https://doi.org/10.3389/fmicb.2018.00274.

Patil, V., Santos, C.N.S., Ajikumar, P.K., Sarria, S., Takors, R., 2021. Balancing glucose and oxygen uptake rates to enable high amorpha-4,11-diene production in

Escherichia coli via the methylerythritol phosphate pathway. Biotechnol. Bioeng. 118, 1317–1329. https://doi.org/10.1002/bit.27655.

Protzko, R.J., Hach, C.A., Coradetti, S.T., Hackhofer, M.A., Magosch, S., Thieme, N., Geiselman, G.M., Arkin, A.P., Skerker, J.M., Dueber, J.E., Benz, J.P., 2019. Genomewide and enzymatic analysis reveals efficient D-galacturonic acid metabolism in the *basidiomycete* yeast *Rhodosporidium toruloides*. mSystems 4 (4). https://doi.org/10.1128/msystems.00389-19 e00389-19.

Protzko, R.J., Latimer, L.N., Martinho, Z., de Reus, E., Seibert, T., Benz, J.P., Dueber, J.E., 2018. Engineering *Saccharomyces cerevisiae* for co-utilization of d-galacturonic acid and d-glucose from citrus peel waste. Nat. Commun. 9, 5059. https://doi.org/10.1038/s41467-018-07589-w.

Rezić, T., Oros, D., Marković, I., Kracher, D., Ludwig, R., Šantek, B., 2013. Integrated hydrolyzation and fermentation of sugar beet pulp to bioethanol. J. Microbiol. Biotechnol. 23, 1244–1252. https://doi.org/10.4014/jmb.1210.10013.

Richard, P., Hilditch, S., 2009. D-Galacturonic acid catabolism in microorganisms and its biotechnological relevance. Appl. Microbiol. Biotechnol. 82, 597–604. https://doi.org/10.1007/s00253-009-1870-6.

Russmayer, H., Egermeier, M., Kalemasi, D., Sauer, M., 2019. Spotlight on biodiversity of microbial cell factories for glycerol conversion. Biotechnol. Adv. 37, 107395. https://doi.org/10.1016/j.biotechadv.2019.05.001.

Souffriau, B., den Abt, T., Thevelein, J.M., 2012. Evidence for rapid uptake of d-galacturonic acid in the yeast *Saccharomyces cerevisiae* by a channel-type transport system. FEBS Lett. 286, 2494–2499. https://doi.org/10.1016/j.febslet.2012.06.012.

Swinnen, S., Ho, P.W., Klein, M., Nevoigt, E., 2016. Genetic determinants for enhanced glycerol growth of *Saccharomyces cerevisiae*. Metab. Eng. 36, 68–79. https://doi.org/10.1016/j.ymben.2016.03.003.

Swinnen, S., Klein, M., Carrillo, M., McInnes, J., Nguyen, H.T.T., Nevoigt, E., 2013. Re-evaluation of glycerol utilization in *Saccharomyces cerevisiae*: characterization of an isolate that grows on glycerol without supporting supplements. Biotechnol. Biofuels 6, 157. https://doi.org/10.1186/1754-6834-6-157.

Taccari, M., Canonico, L., Comitini, F., Mannazzu, I., Ciani, M., 2012. Screening of yeasts for growth on crude glycerol and optimization of biomass production. Bioresour. Technol. 110, 488–495. https://doi.org/10.1016/j.biortech.2012.01.109.

Teleki, A., Sánchez-Kopper, A., Takors, R., 2015. Alkaline conditions in hydrophilic interaction liquid chromatography for intracellular metabolite quantification using tandem mass spectrometry. Anal. Biochem. 475, 4–13. https://doi.org/10.1016/j.ab.2015.01.002.

Thierie, J., Penninckx, M., 2010. Crabtree effect. In: Flickinger, M.C. (Ed.), Encyclopedia of Industrial Biotechnology: Bioprocess, Bioseparation and Cell Technology. Wiley, pp. 1774–1790. https://doi.org/10.1002/9780470054581.eib243.

Tripathi, N., Hills, C.D., Singh, R.S., Atkinson, C.J., 2019. Biomass waste utilisation in low-carbon products: harnessing a major potential resource. npj Climate and Atmospheric Science 2, 1–10. https://doi.org/10.1038/s41612-019-0093-5.

Valk, L., 2020. Microbial and metabolic diversity of anaerobic D-galacturonate fermentation. https://doi.org/10.4233/uuid:b34efe06-28d4-4f4c-9fe1-9d2b1696f111.

Verduyn, C., Postma, E., Scheffers, W.A., van Dijken, J.P., 1992. Effect of benzoic acid on metabolic fluxes in yeasts. Yeast 8, 501–517. https://doi.org/10.1007/BF00270792.

Wendisch, V.F., Meiswinkel, T., Lindner, S., 2011. Use of glycerol in biotechnological application. In: Montero, G., Stoytcheva, M. (Eds.), Biodiesel - Quality, Emissions and By-Products. InTech, Rijeka, pp. 305–340. https://doi.org/10.5772/25338.

Wang, X., Yang, J., Yang, S., Jiang, Y., 2019. Unraveling the genetic basis of fast L-arabinose consumption on top of recombinant xylose-fermenting *Saccharomyces cerevisiae*. Biotechnol. Bioeng. 116, 283–293. https://doi.org/10.1002/bit.26827.

Xiberras, J., Klein, M., de Hulster, E., Mans, R., Nevoigt, E., 2020. Engineering *Saccharomyces cerevisiae* for succinic acid production from glycerol and carbon dioxide. Frontiers in Bioengineering and Biotechnology 8, 566. https://doi.org/10.3389/fbioe.2020.00566.

Yang, F., Hanna, M.A., Sun, R., 2012. Value-added uses for crude glycerol - a byproduct of biodiesel production. Biotechnol. Biofuels 5, 13. https://doi.org/10.1186/1754-6834-5-1322413907.

Yazdani, S.S., Gonzalez, R., 2007. Anaerobic fermentation of glycerol: a path to economic viability for the biofuels industry. Curr. Opin. Biotechnol. 18, 213–219. https://doi.org/10.1016/j.copbio.2007.05.002.

Ye, S., Kim, J.-W., Kim, S.R., 2019. Metabolic engineering for improved fermentation of L-arabinose. J. Microbiol. Biotechnol. 29, 339–346. https://doi.org/10.4014/jmb.1812.12015.

Zimmermann, M., Sauer, U., Zamboni, N., 2014. Quantification and mass isotopomer profiling of α-keto acids in central carbon metabolism. Anal. Chem. 86, 3232–3238. https://doi.org/10.1021/ac500472c.